AN ABSTRACT OF THE THESIS OF

Robert William Legan (Name) for the M.S. (Degree) in Nuclear Engineering (Major)

Date thesis is presented _____

Title FRICTION LOSS AND HEAT TRANSFER CHARACTERISTICS FOR TURBULENT FLOW OF LIQUID-LIQUID DISPERSIONS

Abstract approved [redacted] (Major professor)

The momentum and heat transfer characteristics of liquid-liquid dispersions flowing turbulently in circular tubes were studied. Experiments were conducted to obtain friction factors, and heat transfer coefficients for dispersions of various concentrations of two petroleum oils in water. Most of the previous work on liquid-liquid dispersions has been obtained on a dispersion in which the properties of each phase are similar. There was then a need to study other mixtures in which the properties of the dispersed phase were considerably different from those of the continuous phase. This was the object of this present study.

Friction losses and the heat transfer coefficients were measured in a straight copper tube one inch in outside diameter and 0.823 inches in inside diameter. The test section was vertical and had an overall length of 9-1/2 feet. The studies were conducted over a six-foot section. The fluids used in the present work were a light oil,

viscosity of 15 centipoise, and a heavy oil, viscosity of 200 centipoise. Dispersions of 10, 20, and 35 volume percent of the light oil and 4.5 and 21 volume percent of the heavy oil were investigated. Reynolds numbers ranged in this investigation from 15,000 to140,000.

It was found that the friction factors could be expressed by Blasius' equation for Newtonian fluids. An effective dispersion viscosity was found by fitting the pressure drop and mass flow rate to a 1.75 slope. The following relation was used:

$$\Delta P_f = \frac{L\mu^{0.25}}{133.42\ \rho_e D^{4.75}} W^{1.75}$$

The effective viscosity of the dispersions were obtained for three bulk fluid temperatures. In correlating the heat transfer results to Colburn's equation, the effective viscosity at the film temperature was used to calculate the Reynolds number. The Prandtl number used was that of the continuous phase at the film temperature.

At the high bulk fluid temperature the dispersions friction factors increased sharply at the low flow rates. For the light oil dispersions large deviations were observed from Colburn's equation at the low flow rates. These deviations were attributed to dispersion separation. In general, the friction factor and heat transfer results can be represented by equations applicable to single-phase Newtonian fluids.

FRICTION LOSS AND HEAT TRANSFER CHARACTERISTICS FOR TURBULENT FLOW OF LIQUID-LIQUID DISPERSIONS

by

ROBERT WILLIAM LEGAN

A THESIS

submitted to

OREGON STATE UNIVERSITY

in partial fulfillment of
the requirements for the
degree of

MASTER OF SCIENCE

June 1965

APPROVED:

[redacted]

Professor of Chemical Engineering

[redacted]

Head of Department of Chemical Engineering

[redacted]

Dean of Graduate School

Date thesis is presented [illegible] 5, 1964

Typed by Muriel Davis

ACKNOWLEDGMENTS

I would like to express my grateful appreciation to the following:

To Dr. James G. Knudsen, professor of Chemical Engineering, for posing the problem and for his guidance and assistance during the course of the project.

To the National Science Foundation for financial assistance in the form of a Research Assistantship.

To the Department of Chemical Engineering, J. S. Walton, Head, for the use of its facilities.

To the Department of Statistics for the use of their IBM 1620 computer.

And finally to my wife, Janis, for her love and understanding, especially during the conclusion of this work.

TABLE OF CONTENTS

	Page
INTRODUCTION	1
THEORY AND PREVIOUS WORK	3
Flow of Single-Phase Fluids	3
Turbulent Flow of Non-Newtonian Fluids	10
Two-Phase Flow	11
Heat Transfer to Newtonian Fluids	14
Heat Transfer to Two-Phase Systems and Non-Newtonian Liquids	16
Heat Transfer to Non-Newtonian Fluids	18
EXPERIMENTAL PROGRAM	19
APPARATUS	22
General Description	24
PROCEDURE	27
SAMPLE CALCULATIONS	30
Pressure Drop and Friction Factor	30
Heat Transfer	35
Estimation of Experimental Error	42
DISCUSSION OF RESULTS	47
Friction Factor Data	47
Heat Transfer	67
CONCLUSIONS	77
RECOMMENDATIONS	79
Further Work	79
Apparatus Design Changes	80
BIBLIOGRAPHY	81
APPENDIX	84

LIST OF TABLES

Table		Page
1	Comparison of the Friction-Factor Equations at Various Values of the Reynolds Number	9
2	Summary of Ward's Dropsize	14
3	Summary of Experimental Program	21
4	Effect of Tube Diameter on Flow Constants	32
5	Summary of Estimated Maximum Experimental Error	46
6	Summary of Friction Factor Results Complete Data	50
7	Summary of Friction Factor Results Neglecting Low Flow Rates	51
8	Effective Viscosities at Room Temperature in Turbulent Range of Previous Workers Compared with Pressure Drop Method	66
9	Summary of Heat Transfer Results	73

Appendix Table

10	Observed and Calculated Friction Factor Data	84
11	Observed and Calculated Heat Transfer Data	89
12	Physical Properties of Oils (Ward)	95
13	Density of Manometer Fluids (Ward)	95

LIST OF FIGURES

Figure		Page
1	Schematic Flow Diagram	23
2	Friction Loss vs Mass Flow for Run H21	53
3	Friction Factor Plot	54
4	Friction Factor Plot of L10.4 @ Three Temperatures	55
5	Friction Factor Plot of L18 @ Three Temperatures . .	56
6	Friction Factor Plot of L33 @ Three Temperatures	57
7	Friction Factor Plot of H4.5 @ Three Temperatures	58
8	Friction Factor Plot of H21 @ Three Temperatures	59
9	Ward's Friction Factor Data - Light Oil	60
10	Ward's Friction Factor Data - Heavy Oils	61
11	Relative Fluidities	65
12	Light Oil Heat Transfer Results	69
13	Heavy Oil Heat Transfer Results.	70
14	Faruqui's Heat Transfer Results.	71
15	Variation of Heat Transfer Coefficients with Flow Rate	76

FRICTION LOSS AND HEAT TRANSFER CHARACTERISTICS FOR TURBULENT FLOW OF LIQUID-LIQUID DISPERSIONS

INTRODUCTION

Growing interest in two-phase flow is evidenced by the recent increase in publications dealing with the horizontal and the vertical flow of gas-liquid, liquid-liquid, and liquid-solid mixtures. The flow of both gas-liquid and liquid-liquid mixtures is of importance in petroleum production and transport, while the flow of gas-liquid mixtures is important in chemical reactors, in evaporator design and applications are being encountered in the design of nuclear reactors. The flow of liquid-solid systems is met in certain chemical reactions, in pipeline transport of coal, ores, and other solids and is also of considerable interest in nuclear reactor design.

While much attention has been given to the vertical flow of gas-liquid mixtures, little has been devoted to the fundamentally simpler case of liquid-liquid mixtures. This is undoubtedly because of the greater number of applications of the former case as compared with the latter and especially because of the interest of the petroleum industry. Yet, the vertical flow of a gas-liquid mixture is a special case of the flow of two immiscible fluids--and a complex one because of the compressibility of the gas phase.

The research described in this report is part of a continuing

project being conducted at this University to characterize the momentum and heat transfer properties of liquid-liquid flow systems. Previous work has included determination of effective values of the viscosity for laminar and turbulent flow, and turbulent friction factors, heat transfer coefficients, and velocity and temperature profiles for a dispersion of a commercial light petroleum solvent in water. The petroleum solvent had properties similar to that of water. Thus the above studies at this University were determined for only one system in which the properties of the dispersed and continuous phases were similar.

The object of this study was to measure the friction factors and heat transfer coefficients for the turbulent flow of liquid-liquid dispersions in smooth circular tubes. Two fluids were studied. A light oil having a viscosity of 15 centipoise and a heavy oil having a viscosity of 200 centipoise. The friction factors, from which effective viscosity of the dispersion was determined, and heat transfer coefficients were determined for dispersions of three concentrations of the light oil and two concentrations of the heavy oil. The effective viscosity was used to correlate the pressure drop data on a conventional friction factor plot and to correlate the heat transfer results to Colburn's equation.

THEORY AND PREVIOUS WORK

Flow of Single-Phase Fluids

In fluid flow there are several differential equations which result from the application of various physical laws. In these equations, the independent variables are usually the space co-ordinates x, y, z and time t. The dependent variables are velocity, temperature, pressure, and properties of the fluid. The important differential equations of fluid flow are: (1) The continuity equation based on the law of conservation of mass; (2) The momentum equation based on Newton's second law of motion; and (3) The energy equation based on the law of conservation of energy.

A mass balance on a differential element in space yields the continuity equation

$$\frac{\partial(\rho u)}{\partial x} + \frac{\partial(\rho v)}{\partial y} + \frac{\partial(\rho w)}{\partial z} = -\frac{\partial \rho}{\partial t} \qquad (1)$$

Equation (1) is a mathematical expression of the law of conservation of mass and involves no assumptions. All problems in fluid flow require that the continuity equation be satisfied. If steady-state conditions prevail, all deviates with respect to time are zero, and equation (1) becomes

$$\frac{\partial(\rho u)}{\partial x} + \frac{\partial(\rho v)}{\partial y} + \frac{\partial(\rho w)}{\partial z} = 0. \qquad (2)$$

If a fluid is compressible, the density will vary in space, so equation (2) applies for the steady-state flow of a compressible fluid. For the steady-state flow of an incompressible fluid, as most fluids are, the density is constant and the continuity equation becomes

$$\frac{\partial u}{\partial x} + \frac{\partial v}{\partial y} + \frac{\partial w}{\partial z} = 0 \tag{3}$$

which states that the net rate of volume increase per unit volume at a point in an incompressible fluid must be zero. Equation (3) guarantees that no gaps will occur in the fluid and that the fluid cannot pile up at any point.

The energy equation and momentum equation are used in addition to the continuity equation in analyzing fluid-flow situations. The basic general energy equation for steady, isothermal and incompressible flow is

$$\frac{\Delta P}{\rho} + \frac{\Delta(V^2)}{2g_c} + \frac{g}{g_c}\Delta Z = -\overline{w} - l\overline{w} \tag{4}$$

Equation (4) is frequently referred to as Bernoulli's equation when $\overline{w}$ and $l\overline{w}$ are zero.

For conduit of uniform cross-section, equation (4) can be reduced to

$$\frac{\Delta P}{\rho} + \frac{g}{g_c}\Delta Z = -l\overline{w} \tag{5}$$

Equation (5) is applicable to the steady isothermal flow of an

incompressible fluid in a uniform conduit containing no pumps or turbines.

A large number of experimental determinations on turbulent flow of fluids have led to the following relationship known as the quadratic resistance law

$$F = f\rho V^2/2g_c \tag{6}$$

where F is the resisting force per unit area at the wall of the conduit, and f is a proportionality factor known as the Fanning friction factor. If this relation is made equal to the lost work in Equation (5) one obtains

$$\Delta P + \rho \frac{g}{g_c} \Delta Z = \frac{2fL\rho V^2}{Dg_c} \tag{7}$$

For a horizontal tube this becomes the familiar Fanning equation

$$\Delta P_f = \frac{-2fL\rho V^2}{Dg_c} \tag{8}$$

where ΔP_f = the pressure drop due to friction, lb/ft^2.

Equation (8) could also be written as

$$f = \frac{g_c D}{2\rho V^2} \quad (-dP_f/dx) \tag{9}$$

where dP_f/dx is the pressure gradient due to friction loss.

Experimentation shows that in turbulent flow the head loss varies directly as the length of pipe, the square of the velocity, inversely as the diameter, depends upon the surface roughness of the

interior pipe wall, upon the fluid properties of density and viscosity and is independent of the pressure intensity.

As seen from above the friction factor is not a constant but must depend upon velocity V, diameter D, density ρ, viscosity μ, and certain characteristics of the wall roughness that are signified by ϵ, ϵ' and m. These symbols are defined thus: ϵ is a measure of the size of the roughness projections and has the dimensions of a length; ϵ' is a measure of the arrangement or spacing of the roughness elements and also has the dimensions of a length; m is a form factor, depending upon the shape of the individual roughness elements, and is dimensionless. The term f, instead of being a simple constant, turns out to be a factor that depends upon seven quantities.

$$f = F(V, D, \rho, \mu, \epsilon, \epsilon', m) \tag{10}$$

Since f is a dimensionless factor, it must depend upon the grouping of these quantities into dimensionless parameters. For smooth pipe $\epsilon = \epsilon' = m = 0$, leaving f dependent upon the first four quantities. They can be arranged in only one way to make them dimensionless, namely $DV\rho/\mu$, which is the Reynolds number, that is

$$Re = DV\rho/\mu \tag{11}$$

All friction data for turbulent flow in tubes have been correlated by plotting friction factor versus the Reynolds number. Various

friction factor-Reynolds number relationships have been obtained, all of which predict the friction factor with a fair degree of accuracy.

Some of the first friction data for turbulent flow in smooth tubes were obtained by Reynolds (19); however, he determined the pressure gradient along the tube due to friction and did not report friction factors. Extensive data on various fluids and various sizes of tubes have been obtained since Reynolds' experiments, and in 1913 Blasius (2) analyzed all the data and presented a correlation between the friction factor and the Reynolds number. Most workers had investigated only a relatively short range of Reynolds numbers, and the relation obtained was applicable only over the range studied. Blasius suggested the following expression for the friction factor,

$$f = 0.079\, Re^{-0.25} \tag{12}$$

Equation (12) may be used to predict friction factors with excellent accuracy for Reynolds numbers from 3,000 to 100,000. Subsequent experiments covering wider ranges of Reynolds numbers have shown that the Blasius equation does not predict friction factors accurately for Reynolds numbers above 100,000.

In 1914 Stanton and Pannell (21) conducted extensive experiments in which they investigated the flow of air, water, and oil, covering a range of Reynolds numbers from 10 to 500,000. Following these workers, Nikuradse (17) conducted experiments on the flow of water

in smooth pipes for Reynolds numbers ranging from 4,000 to 3,250,000. Knudsen (13, p. 172) has shown the data of these investigators where the friction factor is plotted versus the Reynolds number. The deviation of the Blasius equation from the experimental data at values of the Reynolds number greater than 100,000 is clearly seen. By means of his own data and those of Stanton and Pannell and other investigators Nikuradse obtained the following relationship between f and Re, which is applicable over the whole range of Reynolds numbers investigated.

$$1/\sqrt{f} = 4.0 \log \mathrm{Re}\sqrt{f} - 0.40 \qquad (13)$$

Equation (13) is the friction factor equation recommended for determining friction factors in smooth tubes.

Von Karman (12) derived a theoretical equation

$$1/\sqrt{f} = 4.06 \log \mathrm{Re}\sqrt{f} - 0.60 \qquad (14)$$

which differs only slightly from equation (13).

An empirical equation relating the friction factor and the Reynolds number was presented by Drew, _et al._ (7).

$$f = 0.0014 + 0.125\ \mathrm{Re}^{-0.32} \qquad (15)$$

Equation (15) is somewhat simpler than Nikuradse's equation and is based on 1,310 experiments covering a Reynolds number range from 3,000 to 3,000,000.

A simpler relationship between the Reynolds number and the friction factor is given in Equation (16). This relationship is used in heat-transfer calculations which make use of the analogy between the transfer of momentum and the transfer of heat.

$$f = 0.046\, Re^{-0.2} \tag{16}$$

Table 1. Comparison of the Friction-Factor Equations at Various Values of the Reynolds Number

Re	Eq(12)	Eq(16)	Eq(13)	Eq(14)	Eq(15)
3,000	0.0107	0.00930	0.0109	0.0109	0.0110
10,000	0.00790	0.00730	0.00772	0.00774	0.00797
100,000	0.00443	0.0046	0.00448	0.00449	0.00456
1,000,000	0.00250	0.00289	0.00291	0.00292	0.00290
10,000,000	0.00140	0.00183	0.00204	0.00202	0.00218

In Table 1, Equations (12), (16), (13), (14), (15) are compared with each other and various Reynolds number. Good agreement is obtained at Reynolds number less than 100,000 but at greater values of the Reynolds number the Blasius equation deviates somewhat from the others. The von Karman equation, which was derived from the velocity-distribution equation, shows excellent agreement with Nikuradse's empirical equation.

Turbulent Flow of Non-Newtonian Fluids

Dodge and Metzner (6) have used dimensional analysis to obtain the various groups involved in the turbulent motion of non-Newtonian fluids in pipes.

For the evaluation of friction factors for turbulent non-Newtonian flow they obtained the equation

$$1/\sqrt{f} = A_{1n} \log (Re\, f^{1-n/2}) + C_n \tag{17}$$

and

$$Re = (D^n V^{2-n} \rho / K) \left(\frac{n}{6n+2}\right)^n 8 \tag{18}$$

By analyzing the experimental friction factor data for non-Newtonian liquids these authors proposed that

$$A_{1n} = 4.0/n^{.75}$$

$$C_n = -0.40/n^{1.2}$$

For Newtonian flow Equation (17) and (18) become (13) and (11) respectively.

Shaver and Merrill (20) have done some experimental work on pseudoplastic liquids. They have measured both friction factors and velocity profiles. They have correlated their friction factor data by

$$f = (0.079)/^5 Re^{\gamma} \tag{19}$$

where

$$\gamma = 2.63/(10.5)^n$$

For $n = 1$ this reduces to Equation (11). Both Dodge and Metzer's and Shauer and Merrill's results show the same trend in friction factors; for a particular Reynolds number the friction factor decreases with n. Maude and Whitmore (14) have studied the turbulent flow of suspension as Newtonian fluids and found that the friction factors obtained were less than those predicted by equation (13). This could be due to pseudo-plastic behavior of the suspension.

Two-Phase Flow

The most general approach to the problem of two-phase flow is to consider the equation of motion separately for each of the two phases and solve these subject to certain boundary conditions. The form of these boundary conditions is at times dependent on the equations of motion themselves. Hadamard (11) used this approach to treat the case of a large single droplet of a heavier liquid falling through a second liquid phase. Even then, some simplifying assumptions were required and the results do not agree well with experimental evidence. Except for these simple cases a treatment of this kind is prohibitive.

In order to simplify the problem for liquid-liquid dispersions, Baron, Sterling, and Schueler (1, p. 106) have suggested that it may be possible to handle some incompressible two-phase systems by the methods already developed for single phase flow. They showed

that dispersions of carbon tetrachloride in water, under turbulent flow conditions, friction factors increased with dispersed phase concentration. Since these curves could be matched with a reference curve for pure water by the assignment of an effective viscosity, it was assumed that the dispersions could be treated as a single-phase fluid.

Baron, et al., considering the inertia forces responsible for the relative acceleration between the dispersed phase and continuous phases proposed that the ratio of these forces be less than unity. Their criterion for treating as liquid-liquid dispersion as a single-phase fluid was

$$(Re)_c \, (dp/D)^2 \, \rho_d/\rho_c < 1 \qquad (20)$$

where dp is the particle diameter.

In considering the motion of a drop relative to a small volume element Ward (22, p. 140-142) concluded that the effective viscosity of the dispersion should be used, and that a suitable criterion for the treatment of liquid-liquid dispersions as a single-phase fluid should exist in the form

$$(Re) \, (dp/D)^2 \, \rho_d/\rho_e < 2 \qquad (21)$$

where dp is the Sauter mean diameter.

Except for the low flow ten percent heavy oil dispersion,

Ward found equation (21) successfully differentiates between the abnormal behavior of the heavy oil dispersions and the effective single-phase behavior of the light oil and solvent dispersions. Equation (21) states that a liquid-liquid dispersion can be treated as a single-phase fluid if the Sauter mean diameter (dropsize) is less than 320 microns at 10^4 Reynolds number and 100 microns at 10^5 Reynolds number.

Ward (22) studied turbulent flow velocity profiles, friction factor, and dropsize of unstable liquid-liquid emulsions using a petroleum solvent, a light oil, and a heavy oil. The oils were the same as studied in the present work. The petroleum solvent was also studied by Cengel, et al. (3) and Faruqui (8). Table 2 contains the average dispersion droplet diameter in microns that Ward obtained. The average droplet diameter, D10X; the Sauter mean diameter, D32X; and the diameter corresponding to the 95^{th} volumetric percentile, DV95 were chosen to represent the measured drop size.

Cengel, et al. (3) have studied the laminar and turbulent flow of unstable liquid-liquid emulsions, using a petroleum solvent having properties similar to that of water. In vertical turbulent flow all dispersions behaved as Newtonian fluids and the measured friction factors were used to calculate effective viscosities. The 35 and 50 percent dispersions in horizontal flow exhibited non-Newtonian characteristics and had effective viscosities considerably higher than the same dispersion in vertical flow. This behavior was believed to

be due to phase separation resulting from the horizontal configuration.

Table 2. Summary of Ward's Dropsize

Run	W	D10X	D32X	DU95
S05	1 to 4	43	62	90
S10	4	70	89	126
S20	1.2	49	63	86
S35	1.0	68	80	109
S50	2.1	140	207	318
L05	1.2 to 3.8	29	59	115
L10	1.3 to 4.0	37	50	95
L20	1.1 to 3.7	51	94	145
L35	1.0 to 3.7	90	128	218
L50	1.0 to 3.6	96	126	215
H05	3.9	34	89	200
H10	1.2 , 3.6	33	160	320
H20	1.3 , 3.6	40	290	576
H27	1.6 , 3.7	52	224	550

Heat Transfer to Newtonian Fluids

A semi-empirical approach to obtain a relation between the heat transfer coefficient and the flow variables of the fluid is based on dimensional analysis. For L/D greater than 60 it is assumed that

$$h = F(D, V, \rho, \mu, Cp, k) \tag{22}$$

From this the dimensionless groups obtained are the

Stanton number, $St = h/CpG$ (23)

Reynolds number, $Re = DV\rho/\mu$ (11)

and Prandtl number, $Pr = Cp\mu/k$ (24)

Experimentally it is found that the exact form of the relationship is

$$(St)Pr^{2/3} = 0.023\ Re^{-0.2} \tag{25}$$

Since

$$St = Nu/RePr$$

where the Nusselt number, Nu, is hD/k equation (25) can be rewritten as

$$NuPr^{-1/3} = 0.023\ Re^{0.8} \tag{26}$$

These two equations are most frequently used for predicting heat transfer coefficients. Equation (25) is called the Colburn equation and equation (26) the Dittus-Boelter equation. The condition on these equations are

$$L/D > 60$$

$$Re > 10,000$$

and $$0.7 < Pr < 100\ .$$

Colburn (5) has correlated the heat transfer coefficient to friction factor by combining equations (25) and (16). The resulting equation is

$$(St)Pr^{2/3} = f/2 = j_H \tag{27}$$

where j_H is called the Colburn j factor for heat transfer.

Metzner and Friend (15) obtained the equation

$$St = \frac{f/2}{1.2 + 11.8\sqrt{f/2}\ (Pr_w - 1)(Pr_w)^{-1/3}} \qquad (28)$$

In this equation the Prandtl number is evaluated at the wall film temperature.

Heat Transfer to Two-Phase Systems and Non-Newtonian Liquids

Most of the research on heat transfer to dispersions is concerned with mixtures of water and steam. Some work has been done on heat transfer to slurries but little has been published on heat transfer to liquid-liquid dispersions.

Orr and Dallavalle (18) studied heat transfer to solid-liquid suspensions and correlated their data by equation (26) all the groups being evaluated with the suspension properties at the bulk temperatures. Since all properties were evaluated at the bulk temperatures they multiplied the right hand side of the equation by a viscosity correction term

$$(\mu_c/\mu_w)^{0.14}$$

Finnigan (10) and Wright (23) have previously done work on heat transfer to liquid-liquid dispersions using a petroleum solvent as the dispersed phase. Finnigan used equation (26) with a Prandtl number exponent of 0.4 to correlate his results. Wright used

equation (25) to correlate his results. Both workers used the dispersion properties to evaluate the Reynolds number, but they used the thermal conductivity of the continuous phase in the Prandtl and Nusselt numbers. There was considerable scatter in their data.

Velocity and temperature profiles for an unstable liquid-liquid dispersion in vertical turbulent flow have been obtained by Faruqui and Knudsen (9). It was concluded that the dispersions could be treated as Newtonian fluids and an effective viscosity for each concentration was determined using the universal velocity distribution for the turbulent core. This viscosity successfully correlated the friction factor data. The temperature profiles indicated that the dispersions behaved as a single-phase fluid with a Prandtl number equal to that of the continuous phase if the properties were evaluated at the film temperature (average of bulk and wall temperatures). The heat transfer coefficients could be correlated with the usual Colburn j_H factor equation using the Prandtl number of the continuous phase at the film temperature and the Reynolds number based on the effective dispersion viscosity. The results of Cengel et al., Faruqui and Knudsen were limited to dispersions in which the organic phase had a viscosity equal to that of the continuous water phase.

Faruqui (8) correlated his results to equation (25). However, like previous workers, he used the effective dispersion viscosity in calculating the Reynolds number which was calculated from velocity

profiles or friction factor data taken at 68°F. No correction was made to adjust the dispersion viscosity to the film temperature. The film temperature is not a constant but changes with each individual run. However, Faruqui also assumed that the film temperature was a constant. This assumption turns out to be not too serious. Correcting for these two assumptions Faruqui's results are shown in Figure 14 with his data in the Appendix.

Heat Transfer to Non-Newtonian Fluids

Metzner and Friend (15) studied the problem of heat transfer to non-Newtonian liquids in turbulent flow. They related the Prandtl number to the Prandtl number at the wall by

$$(Pr/Pr_w) = (16/Re_f)^{1-1/n} (3n + 1)/4n \qquad (29)$$

The Reynolds number for non-Newtonian fluids is defined by equation (18) and the Prandtl number is defined by

$$Pr = (Cp/k)(\mu/D)^{n-1} (K/8)(6 + 2/n)^n \qquad (30)$$

Among the substances they studied were some slurries that behaved pseudo-plastic liquids.

EXPERIMENTAL PROGRAM

The research described in this report is part of a continuing project being conducted at this University to characterize the momentum and heat transfer properties of two phase liquid-liquid flow systems. Previous work has included the viscosity for laminar and turbulent flow, turbulent friction factors, heat transfer coefficients, velocity and temperature profiles, and drop size distribution for a dispersion of a commercial solvent in water.

Turbulent flow studies of a liquid-liquid dispersion made up of water and a dispersed phase with properties similar to water (8; 9) have resulted in values of the effective viscosity and Prandtl number of the dispersion. The results reported by Cengel, et al. (3) and Faruqui and Knudsen (9) have indicated a need to study turbulent flow friction loss and velocity profiles for dispersions in which the discontinuous phase properties (particularly viscosity) is varied so that the effect of these on the effective viscosity of the dispersion may be determined.

Heat transfer studies (8) have resulted in a correlation in which the Prandtl number to be used is that of the continuous phase. This conclusion was reached from a study of turbulent flow temperature profiles. The results were obtained on a dispersion in which the properties of each phase are similar and there was need to study

other mixtures in which the properties of the dispersed phase are considerably different from those of the continuous phase. Therefore, the objective of this investigation was to study the effect of a dispersion in which the discontinuous phase properties (particularly viscosity) differ widely from the continuous phase. Turbulent friction factor data, apparent viscosity, and heat transfer correlations comprised the investigation. Two organic phases were chosen to give a wide range of viscosity: a light oil at 15 centipoise, and a heavy oil at 200 centipoise. Friction losses were measured at three and two dispersed phase concentration (L10, L20, L35, H4.5, H21) respectively for light and heavy oil, and at three bulk temperatures (68°F., 108°F., 140°F.), and at approximately 18 circulating flow rates. Heat transfer data was also taken with the above dispersed phase concentrations at 18 circulating flow rates.

A summary of all the experimental runs is given in Table 3. The following system was used in identifying the runs. The first letter designates the organic phase: L for light oil, and H for the heavy oil. The numbers following L and H signify the actual concentration of the organic phase in volume percent. Thus a run labeled L10 would indicate a light oil dispersion of ten volume percent.

Table 3. Summary of Experimental Program

Dispersed Phase	Nomenclature	Friction Factor	Heat Transfer
Light Oil	L10	18 flow rates between 1-4 lb/sec and at 3 temperatures	18 flow rates between 1-4 lb/sec
	L10.4		
	L18		
	L20		
	L32		
Heavy Oil	H4.5		
	H21		

APPARATUS

A schematic flow diagram of the apparatus used is shown in Figure 1. The liquid-liquid dispersion, consisting of an organic and a water phase, was contained in the supply tank. A turbine pump circulated the dispersion from the bottom of this tank through the test section, a baffle mixer, a heat exchanger and then back to the tank. This equipment had been used by Finnigan (10), Cengel (4), Wright (23), Faruqui (8), and Ward (22).

The organic phases were highly refined oils (Standard of California White Oil Number One and White Oil Heavy). The physical properties of these two liquids have been determined by Ward (22). Table 2, showing his results, is given in the Appendix.

Except for putting a one-half inch cap on the by-pass line, moving the by-pass outlet to the same side as the return line and agitators, and adding a second mixer, the apparatus is the same as that used by Ward (22), Faruqui (8), and Finnigan (10), and a complete description is given by them (8, p. 29-32; 10, p. 59-61; 22, p. 23-29). These changes were necessary to obtain complete mixing of the dispersion at all flow rates and at high temperatures where the light oil dispersion would separate easily. This apparatus was used so that advantage could be taken of the extensive fluid flow and heat transfer properties already measured on this equipment.

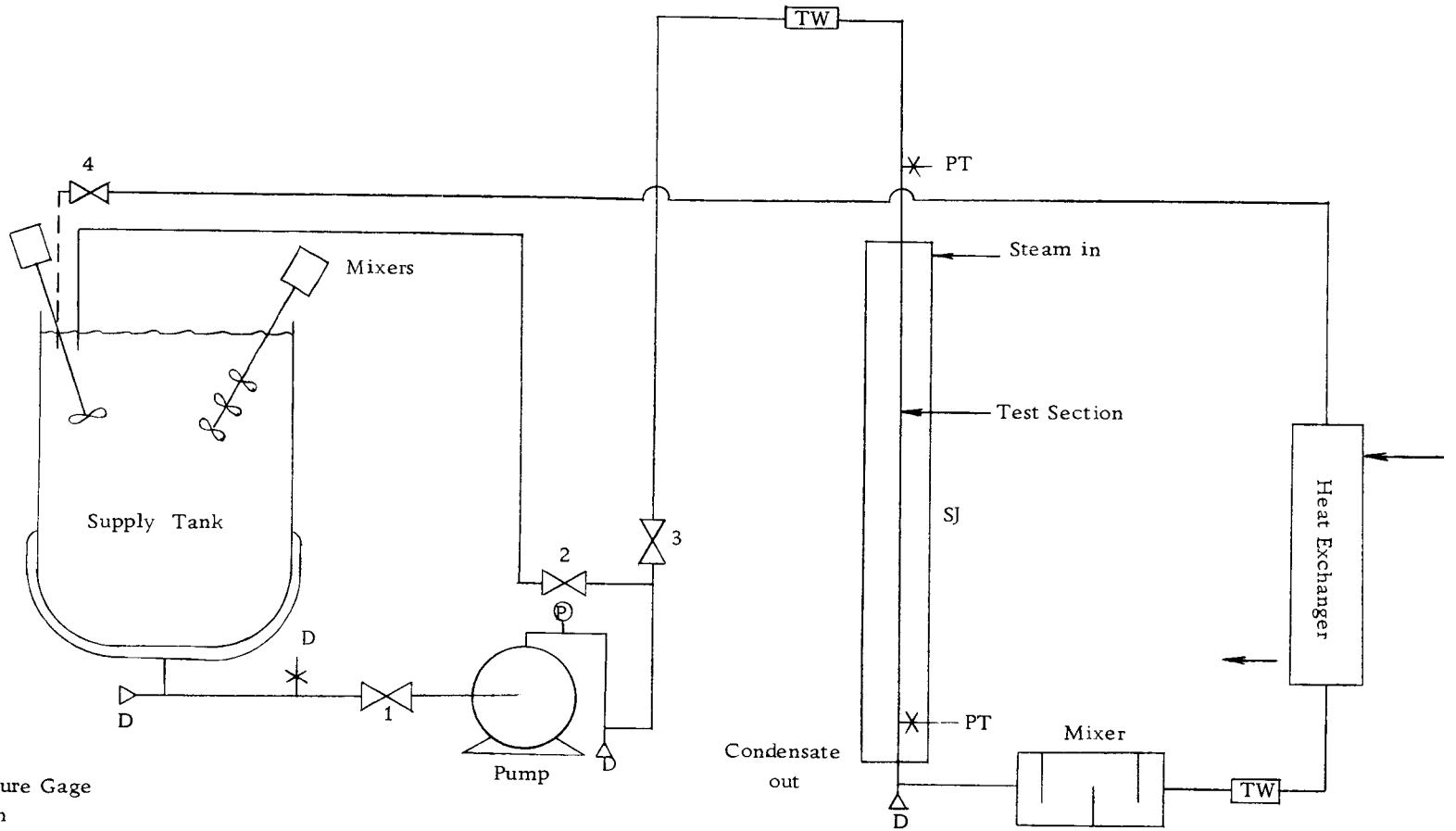

Figure 1. Schematic Flow Diagram

General Description

To minimize corrosion problems all materials contacting the dispersion were either stainless steel, copper, brass, or hard rubber. All the piping system, except the test section was constructed of standard 2-inch and 1-1/4-inch brass pipe. The test section was a 1-inch outside diameter, 0.823-inch inside diameter copper tube 9-1/2 feet long. Pressure tap holes 1/16 inch in diameter were located 2-1/2 feet and 8-1/2 feet from the entrance of the test section for measurement of the friction loss across 6 feet of the test section. This positioning of the pressure taps gave a calming section of 36 diameters before the first static pressure tap. This length is far in excess of 10 diameters predicted by Deissler (13, p. 236-237) for attaining the fully developed friction factor.

The turbine pump, driven by a 1750 RPM three horsepower motor, furnished a steady flow of the dispersion. A flexible hard rubber hose was located at the efflux point of the system to facilitate in diverting the flow to a weighing tank. Valves 2, 3, and 4 (Figure 1) were used to adjust the flow rate through the system.

The friction loss across the six feet of test section was measured by two manometers, one with mercury and the other with a 2.94 specific gravity oil. The manometers were about three feet long and scaled with meter sticks. Copper tubing, 1/4 inch in diameter,

was used as the pressure transmitting line and water was used as the pressure transmitting liquid. About three feet of horizontal liquid tubing was provided at each pressure tap to eliminate the possibility of the dispersion getting into the vertical portion of the tubing. Provision was made for flushing the sensing lines with water. Since the manometer fluid was under water, the effective manometer density used in calculating the pressure loss due to friction was the manometer fluid density minus the density of water. The effective manometer fluid densities are given in the Appendix.

A three-inch standard iron pipe was used as a steam jacket and heated six feet of the test section. The heated section of the tube extended from three feet to nine feet from the entrance to the test section. This provided a calming section of 43 diameters before the dispersion was heated. For turbulent flow at Reynolds number greater than 10,000, Schiller and Kirsten (13, p. 236) observed that entrance lengths greater than 50 tube diameters were generally necessary for the formation of a fully developed turbulent velocity profile. However, it must be assumed in this investigation that for purposes of heat transfer coefficient measurements the velocity profile was fully developed after 43 diameters.

The bulk temperature rise due to heating of the dispersion was measured by two thermometers graduated in 0.1^{o}F. These were placed in the thermometer wells shown in Figure 1. The wall temperature of the heated test section was measured by eight

thermocouples made of 24 gage copper and constantan wire. The thermocouple wire was double-glass wrap, silicone-resin impregnated, high accuracy wire selected to a limit of error of $\pm 1/4^{\circ}F$. This wire was supplied by the Leeds and Northrup Company. Wall thermocouples were soldered in four grooves, two per groove, 1-1/2 inch long and 1/16 inch deep and 1/8 inch wide machined on the outside of the test section wall at distances of 5, 24, 41, and 63 inches from the beginning of the heated section. The thermocouple leads ran along the full length of the test section coming out of the bottom of the steam jacket and going to a Leeds and Northrup (No. 631375) potentiometer with a division of 0.01 millivolt. The potentiometer was used to measure the E.M.F.'s generated.

Since each set of the first three sets of thermocouples differed by as much as $10^{\circ}F$. it is concluded that a new thermocouple design for the measurement of the wall temperature should be investigated for any future work. Mohun and Peterson (16) describes a precision method of embedding thermocouples in a tube wall in order to measure its surface temperature, and they analyze the errors involved in such measurement.

Processing of the friction losses and heat transfer results was done with the aid of an IBM 1620 computer. Program details are given in the section on Sample Calculations and the programs are given in the Appendix.

PROCEDURE

Before each run the system was flushed several times with water and then drained. Flushing was continued until the milky coloring of the water disappeared. When switching from the light oil to the heavy oil, the system was first rinsed with light petroleum solvent and then with water. Water and oil were added to the 80 gallon supply tank in the ratio needed to make a dispersion of the desired concentration. Care was taken to insure that the return hose and by-pass line were maintained under the liquid level at all times. This was done to prevent foaming and to insure that no air was entrained when the liquid returned to the tank. The pump, stirrers, and agitation action of the return fluid were used to mix the two liquids. Ward (22, p.74) showed that equilibrium as evidenced by no change in drop size and distribution was normally established after 200 minutes. In the present study the system was in operation about four hours before any data were taken.

After the four hour period, the manometers were flushed with water to remove any entrained air or oil. When a uniform dispersion had been obtained pressure drop data were commenced. The mass flow rate was adjusted to its maximum value usually about four pounds per second by closing the by-pass line. The manometer deflection, HT, across six feet of the test section and the flow rate

were recorded. The latter was measured by using the hard rubber hose at the end of the return line to divert the flow to a weighing kettle. Then noting the time required to collect a known weight, usually about 100 pounds of the liquid, the dispersion was quickly returned to the supply tank and additional friction factor data were taken at flow rate intervals of 0.2 pounds per second lower until a flow rate of 0.8 pounds per second was reached. This procedure was repeated for three bulk fluid temperatures: 68°F., 108°F., and 140°F. The latter two temperatures were chosen because they were the extreme limits of the film temperature, $T_{0.5}$, as calculated in the heat transfer run for water. Thus, the dispersion viscosities determined at these two temperatures were used to obtain the dispersion viscosities at the other film temperatures for each run. For an example of this method see Sample Calculations. The temperature of the mixture was kept within 1°F. by controlling the cooling water rate or by adjusting the amount of heating time. After the mixture was heated to the desired temperature a few minutes were allowed to pass before the manometer deflections were read. After the data had been taken a two liter sample of the mixture was taken from the return line. The sample was allowed to separate overnight so that the exact concentration of the dispersion could be obtained. To obtain a clear separation of the heavy oil dispersions the samples had to be heated to about 160°F. This was not necessary for the light oil dispersions.

Both manometers were used when possible and the respective friction losses compared. The 2.94 specific gravity oil was out of range above a flow rate of approximately 3.2 pounds per second; this flow changed for each dispersion decreasing with increasing oil concentration. The mercury manometer was not used when the deflection, HT, became less than five centimeters.

At this point the flow was again increased to its maximum value and the heat transfer data taken with this particular emulsion. The cooling water rate and the steam rate were turned on completely so that the change in the fluids temperature at the entrance and exits of test section was a maximum. It was assumed that steady state conditions had been attained when the temperatures TB1 and TB2 did not change by more than 0.2°F. in 15 minutes. It took about 90 minutes from the introduction of steam to reach steady state. Occasionally it was found that the temperatures TB1 and/or TB2 had changed during the reading of the eight thermocouples. This was sometimes caused by a radical change in steam pressure. In this case time was allowed for the system to again stabilize and the data were retaken.

After the heat transfer data were completed the steam was then shut off and when the dispersion had cooled down, the cooling water, stirrers, and pump were shut off.

The observed and calculated data are tabulated in the Appendix.

SAMPLE CALCULATIONS

Pressure Drop and Friction Factor

The pressure drop across the test section, ΔP_T, was calculated from the manometer deflection, HT, and the effective density of the manometer liquid, ρ_m, as follows:

$$-\Delta P_T = K(HT)(\rho_m) \tag{31}$$

where K converts HT from centimeters to feet. Since the test section was vertical with liquids of different densities in the pressure transmission lines and the test section, part of the pressure drop, ΔP_T, was due to the static pressure difference, ΔP_s. If the length of the test section L, the density of the liquid in the test section is ρ_e and the density of the pressure transmission liquid (water) is ρ_w, then

$$\Delta P_s = L(\rho_e - \rho_w) \quad . \tag{32}$$

Since, in this case, dispersions were flowing in the test section, ρ_e was the density of the solvent and water comprising the dispersion. The friction loss, ΔP_f, was then

$$-\Delta P_f = -\Delta P_T + \Delta P_s = K(HT)(\rho_m) + L(\rho_e - \rho_w) \tag{33}$$

The friction factor is calculated by

$$f = \frac{g_c D}{2\rho_e V^2 L} \quad (-\Delta P_f) \tag{34}$$

Since the velocity, V, is related to the mass flow rate, W, by

$$V = 4W/\pi D^2 \rho_e \tag{35}$$

one can write

$$f = \frac{\pi^2 g_c D^5}{32L} \left(\frac{-\Delta P_f}{W^2}\right) \rho_e \tag{36}$$

$$\text{Let} \quad CFF = \pi^2 g_c D^5/32L \tag{37}$$

$$\text{then} \qquad f = CFF\,(-\Delta P_f/W^2)\rho_e \tag{38}$$

The Reynolds number was calculated by

$$Re = 4W/\pi D\mu_e \tag{39}$$

$$\text{or} \qquad Re = CRE\,(W)/\mu_e \tag{40}$$

$$\text{where} \qquad CRE = (1488)\,(12)\,(4)/\pi D \tag{41}$$

and W is expressed as pounds/second, D is the test section inside diameter in inches, and μ_e is the effective viscosity of the emulsion in centipoise.

Using Blasius' equation

$$f = 0.079\, Re^{-.25} \tag{12}$$

and substituting into equation (36) the pressure drop as a function the mass flow rate becomes

$$-\Delta P_f = \frac{(0.079)32L(\mu_e)^{.25}}{4^{.25}\pi^{1.75}D^{4.75}g_c}\left(\frac{W^{1.75}}{\rho_e}\right) \quad (42)$$

or $$-\Delta P_f = \frac{(C175)\,(\mu_e)^{.25}}{\rho_e} W^{1.75} \quad (43)$$

where $$C175 = (0.079)(32)(L)/4^{.25}\pi^{1.75}(D/12)^{4.75}(1488)^{.25}g_c \quad (44)$$

The quantities CRE, CFF, and C175 are functions of diameter only and are listed in Table 4.

Table 4. Effect of Tube Diameter on Flow Constants

Worker	Diameter	CFFx10^6	CRE	C175
Legan	0.823"	2.5094	27,625	2442
Ward	0.826"	2.5555	27,524	2400
Faruqui	0.8275"	2.5788	27,474	2380
Finnigan	0.699"	1.1091	32,525	5304

The following equations were used in this work:

$$f = (2.5094 \times 10^{-6})\left(\frac{-\Delta P_f}{W^2}\right)\rho_e \quad (45)$$

$$-\Delta P_f = 0.032808(HT)\rho_m + 6(\rho_e - \rho_w) \quad (46)$$

$$Re = 27,625\ W/\mu_e \quad (47)$$

and for calculating the viscosity of the dispersion the following equation was used:

$$\Delta P_f = (2442\mu_e^{.25}/\rho_e)\,W^{1.75} \quad (48)$$

The pressure drop, friction factor, Reynolds number, and the dispersion viscosity were calculated and analyzed with the aid of an IBM 1620 digital computer.

For each run, the following information was supplied to the computer: the circulation rate in pounds per second, the manometer deflection, the manometer fluid density, the emulsion density, and the density of water. After calculation of ΔP_f and f the program performed a least squares analysis to find m and b in the equation

$$\text{Log}(\Delta P_f) = m \text{ Log}(W) + b \tag{49}$$

The slope m was then fixed at 1.75 (assuming Blasius' equation) and a new y-intercept was found by a second least squares analysis. This value was then used to calculate an effective viscosity for the dispersion.

Because of emulsion separation at low flow rates, the complete set of data for run L18 had a slope of 1.70 as seen in Table 1. By neglecting these flow rates the slope would approach 1.75. Usually all flow rates below 40,000 Reynolds number had to be neglected. These neglected runs are marked in the Appendix.

The y-intercepts, Y, listed in Table 6 and Table 7 are equal to e^b. Thus the effective emulsion viscosity,

$$\mu_e = [(Y)(\rho_e)/C175]^4 \tag{50}$$

The tabulated friction factor data presented in the Appendix are copies of the computer printout for this program.

A least square analysis of run L18 gave a slope of 1.765, and a Y of 44.5. Fitting the data to a slope of 1.75, Y became 45.3. Then

$$\mu_e = (45.3\rho_e/2442)^4$$

or $$\mu_e = 1.6155 \text{ centipoise} .$$

A sample calculation for run L18 showing the use of equations (45)(46)(47) is given below.

Given: $W = 4.014$ lb/sec

$HT = 20.6$ cm. Hg

temperature dispersion = 70° F.

temperature of manometer board = 72° F.

$\rho_w = 62.30 \text{ lb/ft}^3$

$\rho_s = 53.68 \text{ lb/ft}^3$

therefore,

$$\rho_e = (0.18)(53.68) + (0.82)(62.301) = 60.75 \text{ lbs/ft}^3$$

$$\rho_m = 782.23 \text{ lb/ft}^3$$

$$-\Delta P_f = (0.032808)(20.6)(782.23) + 6(60.75 - 62.30)$$

$$-\Delta P_f = \underline{\underline{519.446 \text{ lb/ft}^2}}$$

$$f = (2.5094 \times 10^{-6})(519.446)(60.75)/4.014^2$$

$$f = \underline{\underline{49.14 \times 10^{-4}}}$$

$$Re = (27625)(4.014)/1.6155 = \underline{\underline{68,637}}$$

Heat Transfer

The average heat transfer coefficient, h, was calculated from the expression

$$q = h A (\Delta T)_m \tag{51}$$

where $(\Delta T)_m$ is the mean temperature difference between the wall and the fluid. The heat transferred, q, was found by the expression

$$q = 3600 W C_{pe} (TB2 - TB1) \tag{52}$$

where C_{pe} the heat capacity of the dispersion was evaluated from the weighted average of the heat capacities of the solvent.

Combining equations (51) and (52)

$$h = \frac{7200}{D\pi} C_{pe} \frac{W(TB2-TB1)}{(\Delta T)_m} \tag{53}$$

for D = 0.823 inches

$$h = 2784.7W(C_{pe})(\Delta T_b / \Delta T_m) \tag{54}$$

where $\Delta T_b = TB2 - TB1$.

The Stanton number was calculated from

$$St = \frac{h}{GC_{pe}} = \frac{h\pi D^2}{14400WC_{pe}} = \frac{D}{288}(\Delta T_b / \Delta T_m) \tag{55}$$

or

$$St = 0.002858 (\Delta T_b / \Delta T_m) . \tag{56}$$

Equation (56) shows that no physical properties were involved in the evaluation of the Stanton number.

The mean temperature difference was evaluated by taking the weighted average temperature difference between the wall and the fluid. For this calculation it was assumed, as approximation, that the temperature rise in the fluid was linear with distance. The thermocouples, T1 and T2 gave the wall temperature at a distance TL1 from the beginning of heating; T3 and T4 gave the temperature at a distance of TL2; T5 and T6 gave the temperature at a distance TL3; T7 and T8 gave the temperature at a distance TL4.

The average temperature of the four sets of thermocouples were called TA, TB, TC, TD. That is TA = (T1 + T2)/2, etc. As an approximation it was assumed that the wall temperature at the start of the heating section was TA and that at the end was TD. Knowing the temperature of the fluid at the beginning and at the end of the test section, the temperature of the fluid at the points TL1, TL2, TL3, TL4 was found by linear interpolation. These temperatures were called, respectively, TM1, TM2, TM3, TM4,

also let

$$TAA = TA - TB1 + TA - TM1$$

$$TBB = TA - TM1 + TB - TM2$$

$$TCC = TB - TM2 + TC - TM3$$

$$TDD = TC - TM3 + TD - TM4$$

$$TEE = TD - TM4 + TD - TB2 \ .$$

The mean temperature was then evaluated by

$$\Delta T_m = \frac{TL1}{2L} TAA + \frac{TL2-TL1}{2L} TBB + \frac{TL3-TL2}{2L} TCC + \frac{TL4-TL3}{2L} TDD + \frac{L-TL4}{2L} TEE . \quad (57)$$

After substituting the numerical values for the various lengths this becomes as follows:

$$\Delta T_m = 0.034722\ TAA + 0.13194\ TBB + 0.11805\ TCC + 0.15278\ TDD + 0.0625\ TEE \quad (58)$$

There was considerable temperature difference between the wall temperatures from the beginning to the end of the heated test section. T1 and T2 were of the order of 200°F. while T7 and T8 were of the order of 165°F. for low flow rates and 140°F. to 100°F. for high flow rates. The temperature difference read by the two thermocouples in the same well, except T7 and T8, was about 10°F. The temperature difference between T7 and T8 was 1° to 2°F.

The Reynolds number was calculated using equation (47). The viscosity of the dispersion at the film temperature, $T_{0.5}$, was determined by pressure drop data and equation (48).

The Prandtl number used was that of the continuous phase, water, at the film temperature. The film temperature used for evaluating the Prandtl number and the dispersion viscosity was

$$T_{0.5} = \frac{T_w + T_b}{2}$$

i.e., it is the arithmetic average of the wall and bulk temperatures.

Since, $$T_b = \frac{TB1 + TB2}{2}$$

and $$T_w = \Delta T_m + T_b$$

therefore, $$T_{0.5} = \frac{\Delta T_m + TB1 + TB2}{2} \qquad (59)$$

The heat transfer data processing was also accomplished by means of the IBM 1620 computer. Input data included the eight thermocouple readings of the wall temperature, the emulsion inlet and outlet bulk temperature, the mass flow rate, and the emulsion heat capacity. This primary program determined the Stanton number, the heat transfer coefficient, and the wall film temperature. After these primary calculations a secondary program was written. The Prandtl number for water, and the emulsion viscosity were determined from $T_{0.5}$. The input data to the secondary program was then the Reynolds number, the Stanton number, and the Prandtl number. After calculating $(St)(Pr)^{2/3}$ the program performed a least square analysis to find $m + b$ in the equation

$$(St)Pr^{2/3} = b\,Re^{m} \qquad (60)$$

m and b were then compared with Colburn's correlation (5). The slope m was then fixed at -0.20 and a new y-intercept was found by a

second least square analysis. This value was then compared with Colburn's value of 0.023. This comparison is made in Table 9. Because the light oil separated at lower flow rates (Reynolds number less than 50,000) these runs were neglected in the least squares analysis.

An example showing the numerical calculation of the heat transfer coefficient, the Stanton number, and the Reynolds number is given below. The dispersion considered is H21. The observed data were: W = 2.072 lbs/sec , TB1 = 81.1°F., TB2 = 98.5°F., T1 = 161°F., T2 = 149.5°F., T3 = 165°F., T4 = 164°F., T5 = 144°F., T6 = 134°F., T7 = 103°F., and T8 = 102°F.

TM1 = TB1 + (ΔT_b)TL1/72
= 81.1 + (98.5 - 81.1)5/72 = 82.3°F.

TM2 = TB1 + (ΔT_b)TL 2/72
= 81.1 + (17.4) 24/72 = 86.9°F.

TM3 = TB1 + (ΔT_b) TL3/72
= 81.1 + (17.4) 41/72 = 91.0°F.

TM4 = TB1 + (ΔT_b) TL4/72
= 81.1 + (17.4) 63/72 = 96.3°F.

TA = (161 + 149.5)/2 = 155.25°F.

TB = (165 + 164)/2 = 164.5°F.

TC = (144 + 134)/2 = 139°F.

TD = (103 + 102)/2 = 102.5°

TAA = 155.25-81.1+155.25-82.3 = 147.1°F.

TBB = 155.25-82.3+164.5-86.9 = 150.55°F.

$$TCC = 164.5 - 86.9 + 139 - 91 = 125.6°F.$$

$$TDD = 139 - 91 + 102.5 - 96.3 = 54.2°F.$$

$$TEE = 102.5 - 96.3 + 102.5 - 98.5 = 10.2°F.$$

Using equation (58)

$$\Delta T_m = (0.034722)(147.1) + (0.13194)(150.55) + (0.11805)(125.6) + (0.15278)(54.2) + (0.0625)(10.2)$$

$$= 5.10 + 19.85 + 14.83 + 8.28 + 0.64 = 48.70$$

$$\Delta T_b = TB2 - TB1 = 17.4.$$

For H21

$$\rho_e = (0.21)(55.22) + (0.79)(62.316) = 11.596 + 49230 = 60.826 \text{ lb/ft}^3$$

or Run H21 is (11.596/60.826)100 or 19% by weight oil. Therefore,

$$C_{pe} = (0.81)(.997) + (0.19)(0.442) = 0.892 \frac{\text{Btu}}{\text{lb°F.}}$$

Using equation (54),

$$h = (2784.7)(2.072)(0.892)(17.4)/48.7 = \underline{\underline{1838.5 \frac{\text{Btu}}{\text{hr, ft}^2\text{, °F.}}}}$$

Using equation (56),

$$St = (0.002858)(17.4)/48.7 = \underline{\underline{1.020 \times 10^{-3}}}$$

The film temperature, $T_{0.5}$ is by equation (59)

$$T_{0.5} = (48.7 + 81.1 + 98.5)/2 = 114.1°F.$$

The Prandtl number of water at 114.1°F. is 3.91. Therefore,

$$(St)(Pr)^{2/3} = (1.020 \times 10^{-3})(3.91)^{2/3} = \underline{\underline{2.53 \times 10^{-3}}}$$

Using Colburn's analogy,

$$(St)Pr^{2/3} = f/2 = j_H$$

$$j_H = 2.531 \times 10^{-3}$$

and $$f/2 = 2.627 \times 10^{-3}$$ (from pressure drop data).

To calculate the Reynolds number the dispersions viscosity at the film temperature must be known. To approximate this viscosity pressure drop data data for all were taken at three bulk dispersion temperatures: 68°F., 103°F., and 130°F. The viscosity at these temperatures of the dispersion was found by the previous discussed method to be 1.1679, 0.8640, and 0.7684 centipoise respectively. Assuming that the logarithm of the viscosity in centipoises versus the logarithm of the absolute temperature (°R) is a straight line, the viscosity of run H21 as a function of temperature is

$$\text{Log}(\mu_e) = -2.64244 \text{ Log } (°R) + 7.26801$$

using this equation

$$\mu_e \text{ @ } 114.1°F. = 0.8228 \text{ centipoises.}$$

Therefore the Reynolds number can now be calculated by equation (47),

$$Re = (27,625)(2072)/0.8228 = \underline{\underline{69,564.}}$$

Estimation of Experimental Error

The experimental errors involved in calculating the various quantities given above can be estimated by the theory of propogation.

Starting with the pressure drop due to friction

$$-\Delta P_f = (0.032808)(HT)(\rho_m) + 6(\rho_e - \rho_w).$$

Assume the error in HT, S_{HT}, is 0.2 cm.

$$S_{PM} = 0.07 \text{ lb/ft}^3$$

$$S_{(PE-PW)} = 0.2 \text{ lb/ft}^3$$

$$S_{PF}^2 = .032808^2 \rho_m^2 S_{HT}^2 + .032808^2 HT^2 S_{PM}^2 + 6 S_{(PE-PW)}^2$$

For the same run L18 @ 4.014 lbs/sec,

$$S_{PF}^2 = .032808^2[(782.23^2)(.2)^2 + (20.6)^2(.07)^2] + (6)(.2)^2$$

$$S_{PF}^2 = 26.34 + 0.002 + 0.24 = 26.58$$

$$S_{PF} = 5.14 \text{ lb/ft}^2.$$

Note that most of the error originates from the error in reading the manometers. Therefore,

$$\Delta P_f = 519.37 \pm 5.14 \text{ lb/ft}^2$$

a 1% error in ΔP_f.

Assuming an error in the total weight of fluid of 0.25 lbs. and an error in the stop watch of 0.1 sec.

$$S_W^2 = (4)\left[\left(\frac{0.25}{100}\right)^2 + \left(\frac{0.1}{25}\right)^2\right]$$

$$S_W^2 = 4 \times 10^{-3}\,(6.25 + 16)$$

$$S_W \doteq 0.019 \text{ lb/sec}$$

Therefore, $W = \underline{4.014 \pm 0.020}$ a 1/2% error in W.

Calculating a standard deviation of the measured value of the test section diameter it becomes,

$$D = 0.823 \pm 0.002 \text{ inches.}$$

Using equation (36)

$$f = \frac{\pi^2 g_c}{32L} D^5 \rho_e (\Delta P_f)/W^2$$

or

$$f = 6.64617 \times 10^{-6}\, D^5 \rho_e\, \Delta P_f / W^2.$$

Setting $S_D = 0.002$

$S_{PE} = 0.2$

$S_W = 0.020$

$S_{PF} = 5.14$

$$S_f^2 = \left(\frac{f}{D}\right)^2 S_D^2 + \left(\frac{f}{\rho_e}\right)^2 S_{PE}^2 + \left(\frac{f}{\Delta P_f}\right)^2 S_{PF}^2 + \left(\frac{2f}{W}\right)^2 S_W^2$$

$$= (3.57 + 2.62 + 23.65 + 23.99)10^{-10} = 53.83 \times 10^{-10}$$

$$S_f = 7.34 \times 10^{-5}$$

or $f = \underline{0.004914 \pm 0.000073}$ a 1-1/2% error in the friction factor.

As seen above the error in the friction factor results from the error in ΔP_f and W. The error in the test section's diameter, and the error in the emulsion density are negligible.

Calculating the error in the Reynolds number is as follows:

$$Re = (22,735)\, W/D\, \mu_e$$

Assume $S_\mu = 0.05$ centipoise

$$S_{Re}^2 = \left[\frac{Re}{W}\right]^2 S_W^2 + \left[\frac{Re}{D}\right]^2 S_D^2 + \left[\frac{Re}{\mu}\right]^2 S_\mu^2$$

$$S_{Re}^2 = 116,964 + 27,822 + 4,511,376 = 4,656,162$$

$$S_{Re} = 2,160$$

Therefore, $Re = \underline{\underline{68,637 \pm 2,160}}$ an error of 3.15% due largely to the uncertainty of the viscosity.

The variables involved in calculating the heat transfer coefficient and the Stanton number are W, ΔT_b, ΔT_m. The error in measuring W was, as stated before, of the order of 1/2%. The error in ΔT_b was of the order of 0.14° F. The error in TM1, TM2, TM3, and TM4 are approximately 0.1°F. Assume $S_{TA}=S_{TC}=5°F.$, $S_{TB} = 10°F.$, and $S_{TD} = 1°F.$ The error in TAA, TBB, TCC, TDD, and TEE are respectively 7°F., 11°F., 11°F., 5°F., and 1.5°F.

The error in the mean temperature difference because of the

uncertainty of the thermocouples is then

$$S_{\Delta T_m}^2 = (.034722 \times 7)^2 + (.13194 \times 11)^2 + (0.11805 \times 11)^2 + (15278 \times 5)^2 + (.0625 \times 1.5)^2$$

$$= .059 + 2.10 + 1.69 + 0.57 + 0.01 = 4.43$$

$$S_{\Delta T_m} = 2.1°F.$$

Therefore $(\Delta T)_m = 48.7 \pm 2.1°F.$ a 4.3% error in $(\Delta T)_m$

Since

$$h = \frac{7200}{\pi D} (C_{pe}) W \Delta T_b / (\Delta T)_m$$

consider the error in D, W, ΔT_b, and $(\Delta T)_m$ respectively then

$$S_h^2 = \left[\frac{h}{D}\right]^2 S_D^2 + \left[\frac{h}{W}\right]^2 S_w^2 + \left[\frac{h}{\Delta T_b}\right]^2 S_{\Delta T_b}^2 + \left[\frac{h}{\Delta T_m}\right]^2 S_{\Delta T_m}^2$$

$$= 20 + 79 + 112 + 6273 = 6484$$

$$S_h = 80 \text{ BTU/hr. ft}^2, °F.$$

then $h = \underline{\underline{1840 \pm 80 \text{ BTU/hr, ft}^2, °F.}}$ a 4.34% error in the heat transfer coefficient. This error is due almost entirely to the uncertainty in the thermocouples measured temperatures.

The error in the Stanton number is then

$$St = \frac{D}{288} (\Delta T_b / \Delta T_m)$$

$$S_{St}^2 = \left[\frac{St}{D}\right]^2 S_D^2 + \left[\frac{St}{\Delta T_b}\right] S_{\Delta T_b}^2 + \left[\frac{St}{\Delta T_m}\right]^2 S_{\Delta T_m}^2$$

$$S_{St}^2 = (6.1 + 67.4 + 1934.5) 10^{-12}$$

$S_{St} = 0.000045$

Therefore

$St = \underline{\underline{0.001020 \pm 0.000045}}$ a 4.4% error in the Stanton number.

Table 5. Summary of Estimated Maximum Experimental Error

Function	Error	Major contributing factors
PF	1%	99% due to S_{HT}
W	1/2%	Stopwatch
f	1-1/2%	ΔP_f and W
Re	2.15%	97% due to S_{μ}
h	4.34%	97% due to $S_{\Delta T_m}$
St	4.4%	96% due to $S_{\Delta T_m}$
$1/\sqrt{f}$	3/4%	
$Re\sqrt{f}$	3-1/4%	

DISCUSSION OF RESULTS

Friction Factor Data

To determine if the apparatus was operating properly, friction factor data for water were obtained. The results, see Figure 3, show good agreement with Blasius' equation. Therefore, it was concluded that the apparatus, as well as the author's experimental technique, were satisfactory.

Friction factor data were taken for liquid-liquid dispersions composed of 10, 20, and 35 volume percent light oil and 4.5, and 21 volume percent heavy oil. These dispersions were also investigated by Ward (22). Ward's friction factor results, Figures 9 and 10, were about three percent higher than those predicted by Nikuradse's equation (equation 13). The curve obtained by Faruqui working on liquid-liquid dispersions composed of water and a petroleum solvent was about two percent higher than equation (13). The difference between their data and equation (13) was attributed to the difficulty in measuring average diameter of the test section. This explanation is quite feasible since the measured friction factor is proportional to the fifth power of the diameter, [equation (36)]. Baron, et al. (1, p. 121) found experimentally that friction factors slightly higher than those predicted by equation (13) are typical of small diameter

pipe. Therefore, to correlate the friction factors so liquid-liquid dispersion viscosities could be obtained, an effective diameter of the test section was found.

By examining equation (48) it is seen that by plotting $\log \Delta P_f$ versus $\log W$ a straight line will result. This plot should have a slope of 1.75, assuming Blasius' equation holds, and a y-intercept that is proportional to the fluid viscosity to the 0.25 power and to the diameter to the -4.75 power. Since the viscosity of water is well known an effective diameter of the test section could be obtained by determining the y-intercept of the above plot for water. Once the effective diameter of the test section is obtained a similar plot or procedure can be used on fluids, in this case liquid-liquid dispersions, to obtain their effective viscosity. This was the procedure used in this report in analyzing the friction-factor data. This procedure appears to be superior to the previous methods of Cengel et al (3), Faruqui and Knudsen (9), and Ward (22) because the results show less scatter. The experimental error in ΔP_f and W were much smaller than other quantities as Table 5 shows. Table 6 contains a summary of the slope, y-intercept, effective viscosity, and the relative viscosity, μ_e/μ_w, for all runs. These values were obtained from a least square analysis of equation (48). The friction factor data can be seen on Figures 3 through 8.

The effective diameter of the test section calculated from the water friction losses was 0.823 inches. Faruqui (8) reported a measured diameter of 0.830 ± 0.004 inches. By applying the above procedure to Faruqui's data an effective diameter of 0.8275 inches was obtained. This effective diameter is in excellent agreement with his reported average diameter. The effective diameter of the same test section by applying Ward's data was 0.826 inches. A gradual reduction of the effective diameter is seen to have taken place over a period of five years. Finnigan (10) also working with this apparatus but using a different test section reported a diameter of 0.700 inches. By applying equation (48) to his data an effective diameter of 0.699 inches was obtained. It was concluded in the light of the above results that the effective diameter of the test section could successfully be predicted by equation (48).

Once having determined the effective diameter of the test section, 0.823 inches, equation (48) was used in determining effective viscosity of the dispersion. The effective viscosities determined in this manner are shown in Tables 6 and 7. A least square analysis on the data shows an average error of 1/3 percent on the slope and 1/2 percent on the y-intercept. This indicates that the appratus was operating satisfactorily. The fact that the slopes in Table 7 approach 1.75 indicates, in general, that the liquid-liquid dispersions investigated followed Blasius' equation and can be represented as

Table 6. Summary of Friction Factor Results Complete Data

			Slope = 1.75		
Run(Temp)	Slope	Y-intercept	Y-intercept	Viscosity	μ_e/μ_c
Water (72)	1.764±.004	38.4±.1	38.8	0.9578	1.01
L10(68)	1.750±.006	42.2±.2	42.2	1.2712	1.27
L10.4(68)	1.752±.005	43.9±.2	44.0	1.5018	1.50
L10.4(108)	1.719±.007	42.2±.3	41.1	1.1025	1.77
L10.4(140)	1.69±.01	42.4±.5	40.2	0.9832	2.10
L18 (70)	1.705±.005	47.7±.2	46.1	1.7260	1.76
L18 (108)	1.72±.01	44.0±.4	42.8	1.2418	1.99
L18 (140)	1.63±.01	46.0±.5	41.9	1.0998	2.35
L20 (68)	1.703±.006	47.3±.2	45.8	1.6860	1.70
L33 (70)	1.730±.005	50.9±.2	50.1	2.2159	2.28
L33(108)	1.70±.01	48.3±.5	46.5	1.5838	2.52
L32(140)	1.58±.02	52 ± 1	47.0	1.6055	3.42
L35 (68)	1.78±.01	48.3±.5	49.4	2.1098	2.11
H4.5 (68)	1.750±.006	41.5±.2	41.5	1.2288	1.23
H4.5(108)	1.727±.008	39.3±.3	38.5	0.8829	1.41
H4.5(140)	1.688±.009	39.9±.3	37.8	0.7962	1.70
H21 (68)	1.710±.007	43.3±.3	41.9	1.1861	1.19
H21(103)	1.69±.01	41.6±.5	39.4	0.9031	1.36
H21(130)	1.60±.02	44.3±.6	39.6	0.8956	1.75

Table 7. Summary of Friction Factor Results Neglecting Low Flow Rates

Run(Temp)	Slope	Y-intercept	Slope = 1.75 Y-intercept	Viscosity	μ_e/μ_c
Water(72)	1.78±.01	37.6±.6	39.0	0.9770	1.03
L10 (68)	1.777±.008	41.0±.4	42.1	1.2607	1.26
L10.4 (68)	1.767±.006	43.3±.2	44.0	1.4994	1.50
L10.4(108)	1.754±.008	40.6±.3	40.8	1.0760	1.73
L10.4(140)	1.74±.01	40.1±.4	39.8	0.9446	2.01
L18 (70)	1.765±.007	44.5±.4	45.3	1.6155	1.65
L18(108)	1.756±.008	42.2±.3	42.5	1.2079	1.94
L18(140)	1.80±.01	38.7±.5	40.8	0.9917	2.12
L20 (68)	1.724±.007	46.2±.3	45.0	1.5712	1.58
L33 (70)	1.739±.008	50.4±.4	49.9	2.1804	2.24
L33(108)	1.73±.02	46.9±.7	46.1	1.5266	2.43
L32(140)	1.73±.01	45.0±.5	44.3	1.2596	2.69
L35 (68)	1.75±.01	50.1±.5	50.1	2.2297	2.23
H4.5 (68)	1.750±.005	41.4±.2	41.4	1.2171	1.22
H4.5(108)	1.759±.006	38.0±.2	38.3	0.8672	1.39
H4.5(140)	1.729±.008	38.3±.3	37.5	0.7696	1.64
H21 (68)	1.749±.007	41.8±.3	41.7	1.1679	1.17
H21(103)	1.745±.006	39.2±.2	39.0	0.8640	1.30
H21(130)	1.74±.01	38.6±.5	38.2	0.7684	1.50

single-phase Newtonian fluids.

However, by observing Figure 2 and Table 6, deviation from a 1.75 slope is evident for the liquid-liquid dispersions at the higher bulk temperature and at lower flow rates. Figure 2 shows that this deviation for dispersion H21 at 130°F. begins at 1.5 pounds/second and increases with decreasing flow rate. Note that almost no deviation is observed at the low flow rates for the same run at 68°F. By neglecting these low flow rates as was done in compiling Table 7 a slope of 1.74 ± 0.1 was obtained for run H21 at 130°F. instead of 1.60 ± 0.02 which was observed for the complete set of data. The liquid-liquid dispersions were unstable at room temperature but as the temperature was increased more agitation in the supply tank was required to keep the dispersion mixed. At these high temperatures and low flow rates the dispersion apparently was not a homogeneous mixture; and thus the viscosity is a function of the flow rate and degree of separation in this region. For example, the effective viscosity of H21 at 130°F. was 0.77 centipoise, Table 7; however, by fitting the friction factor at 0.671 pounds/second to Blasius' equation the effective viscosity would be 2.5 centipoise. This characteristic of flow rate dependency on the effective viscosity was also reported by Cengel, et al. (3). Cengel (4, p. 66) obtained for the dispersion S50 an effective viscosity of 5.0 centipoise at 3.5 pounds/second and 9.4 centipoise at 0.5 pounds/second.

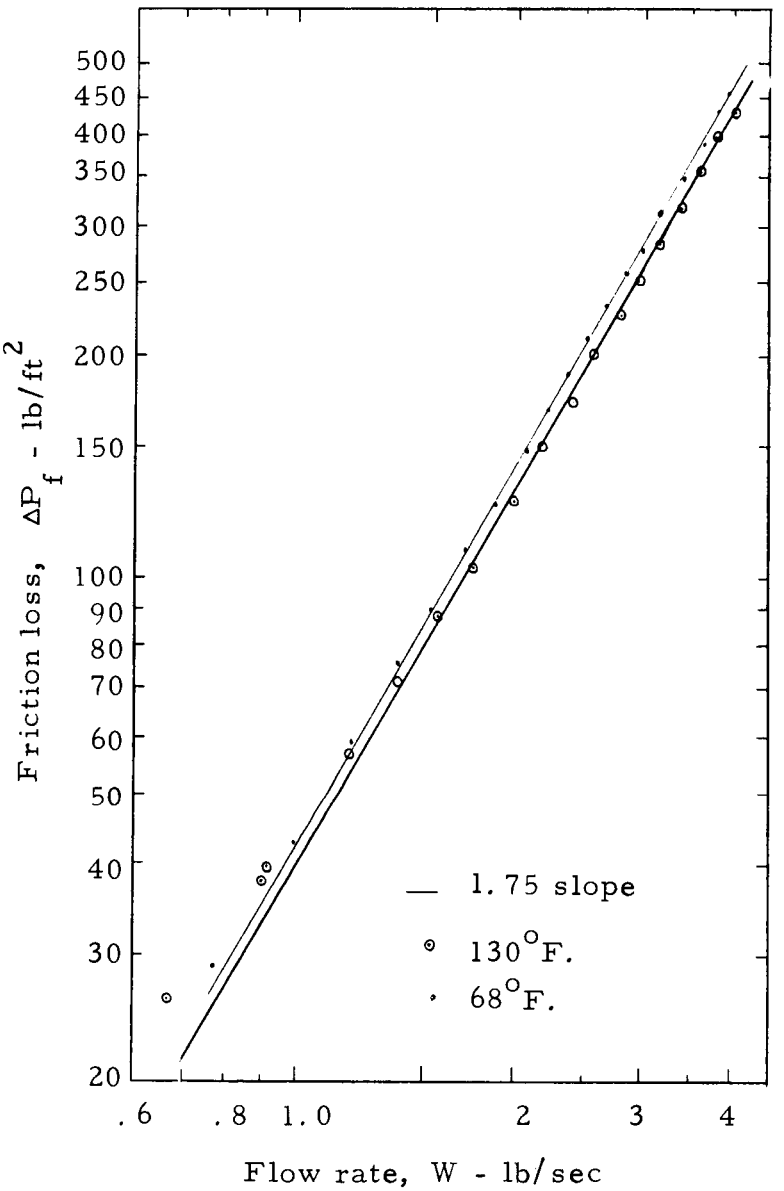

Figure 2. Friction Loss vs Mass Flow for Run H21

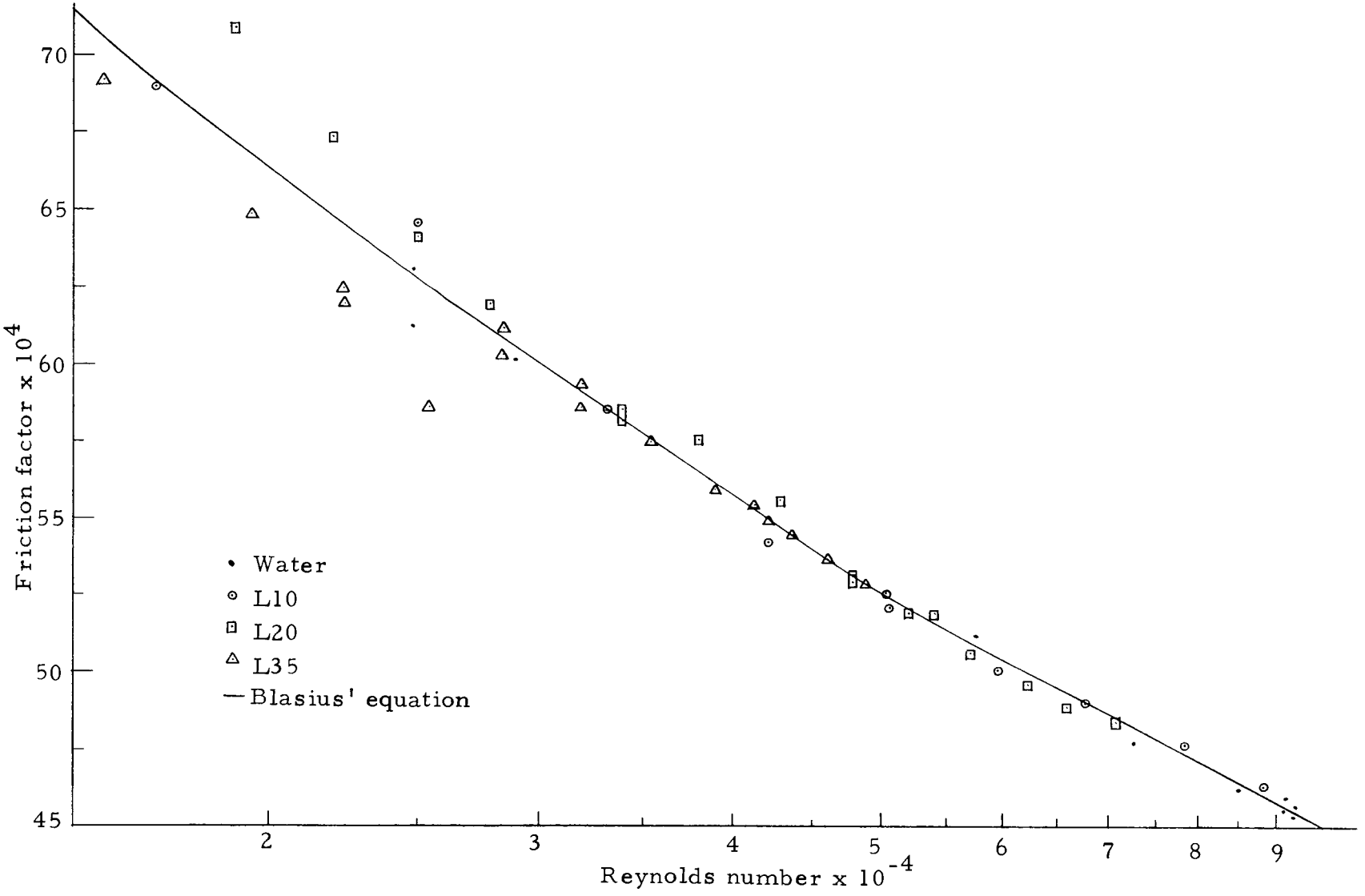

Figure 3. Friction Factor Plot

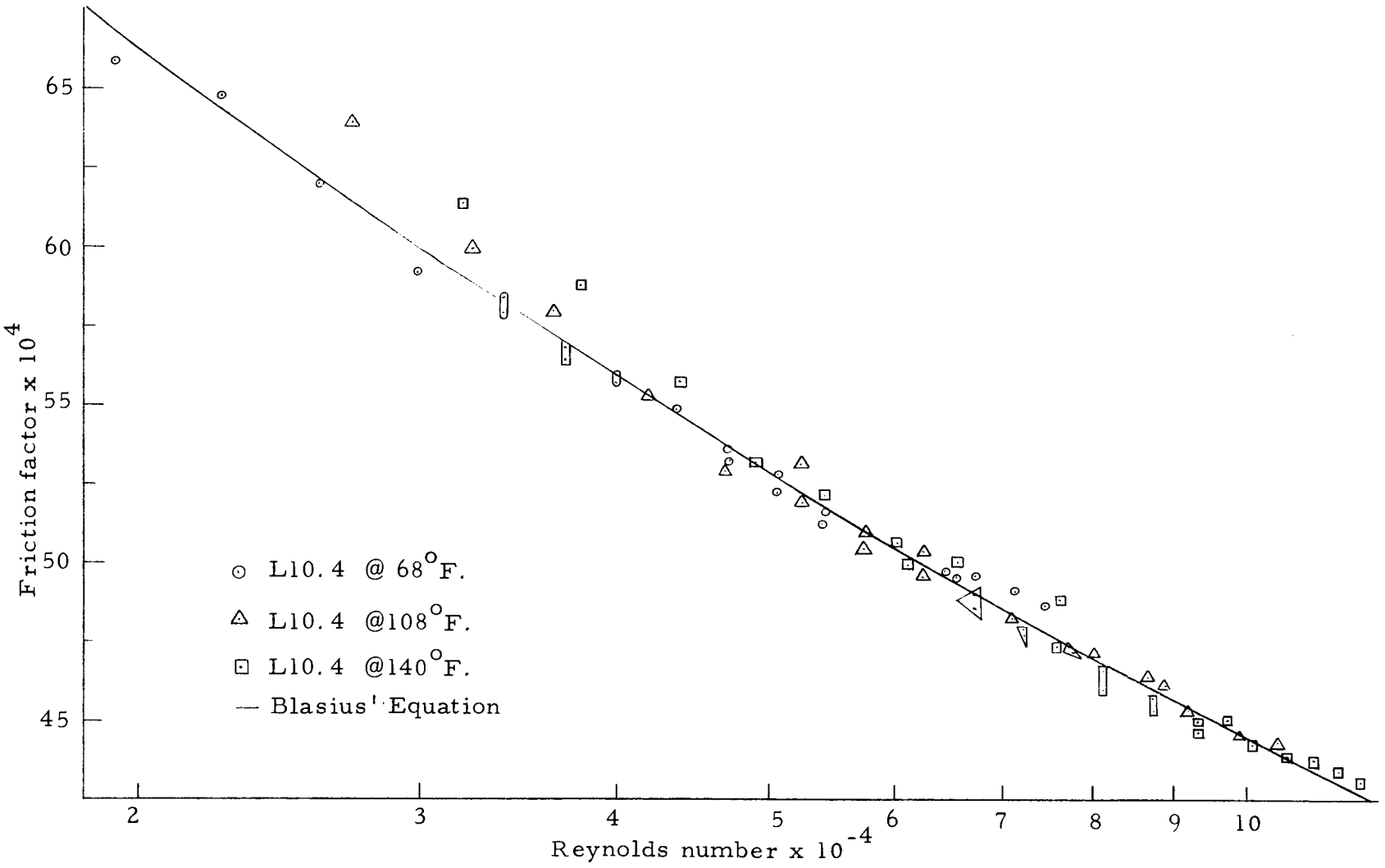

Figure 4. Friction Factor Plot of L10.4 @ Three Temperatures

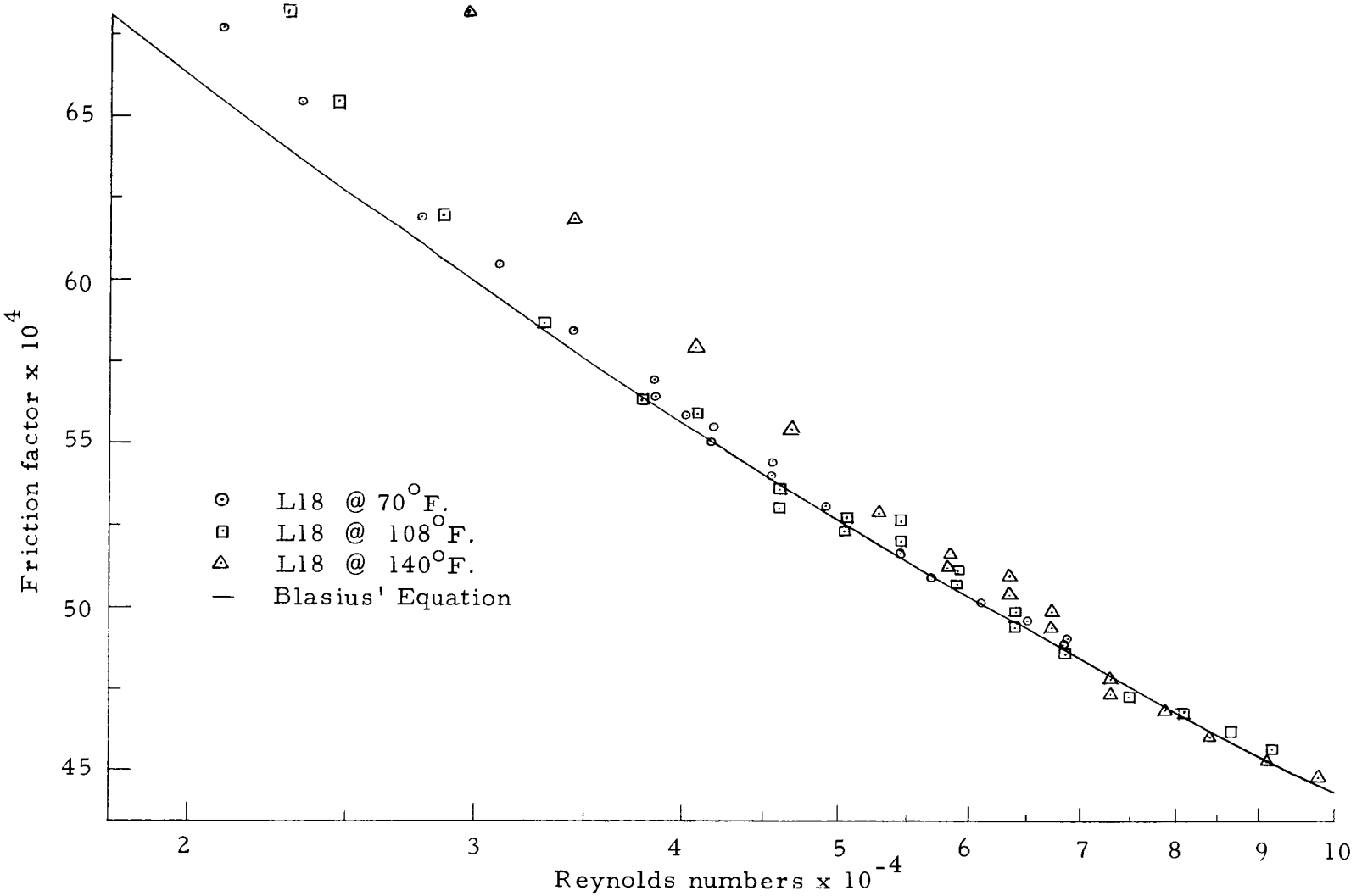

Figure 5. Friction Factor Plot of L18 @ Three Temperatures

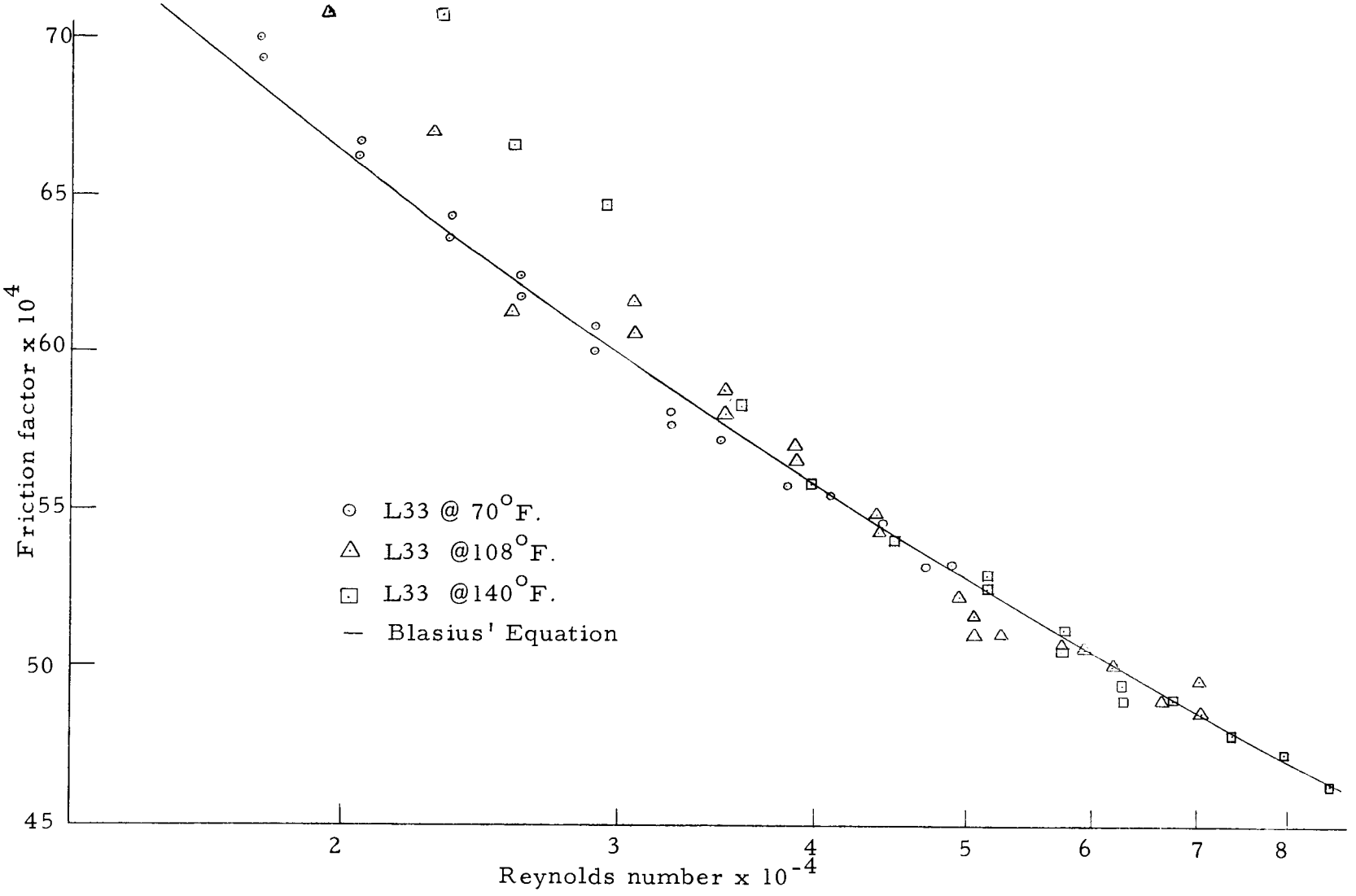

Figure 6. Friction Factor Plot of L33 @ Three Temperatures

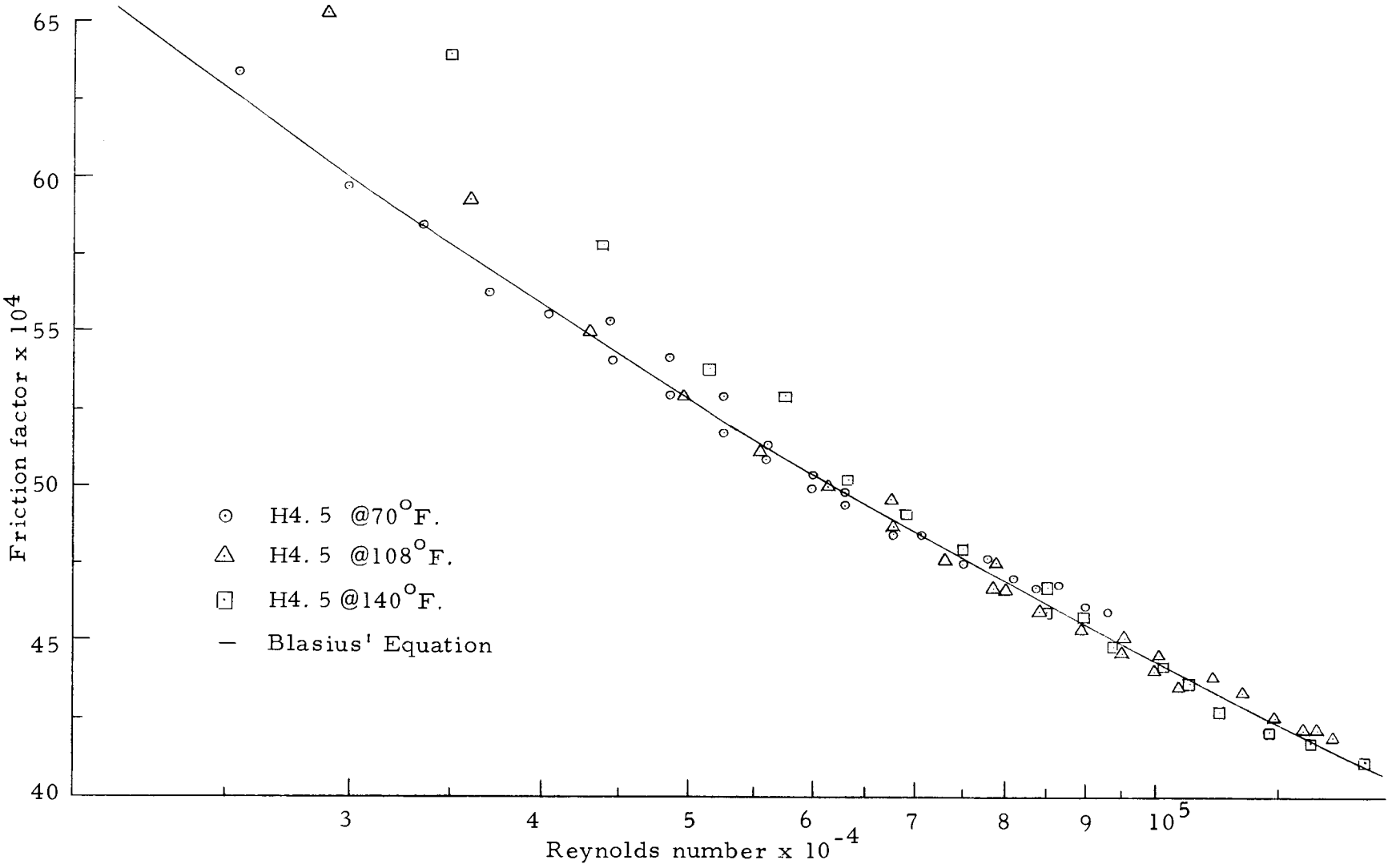

Figure 7. Friction Factor Plot of H4.5 @ Three Temperatures

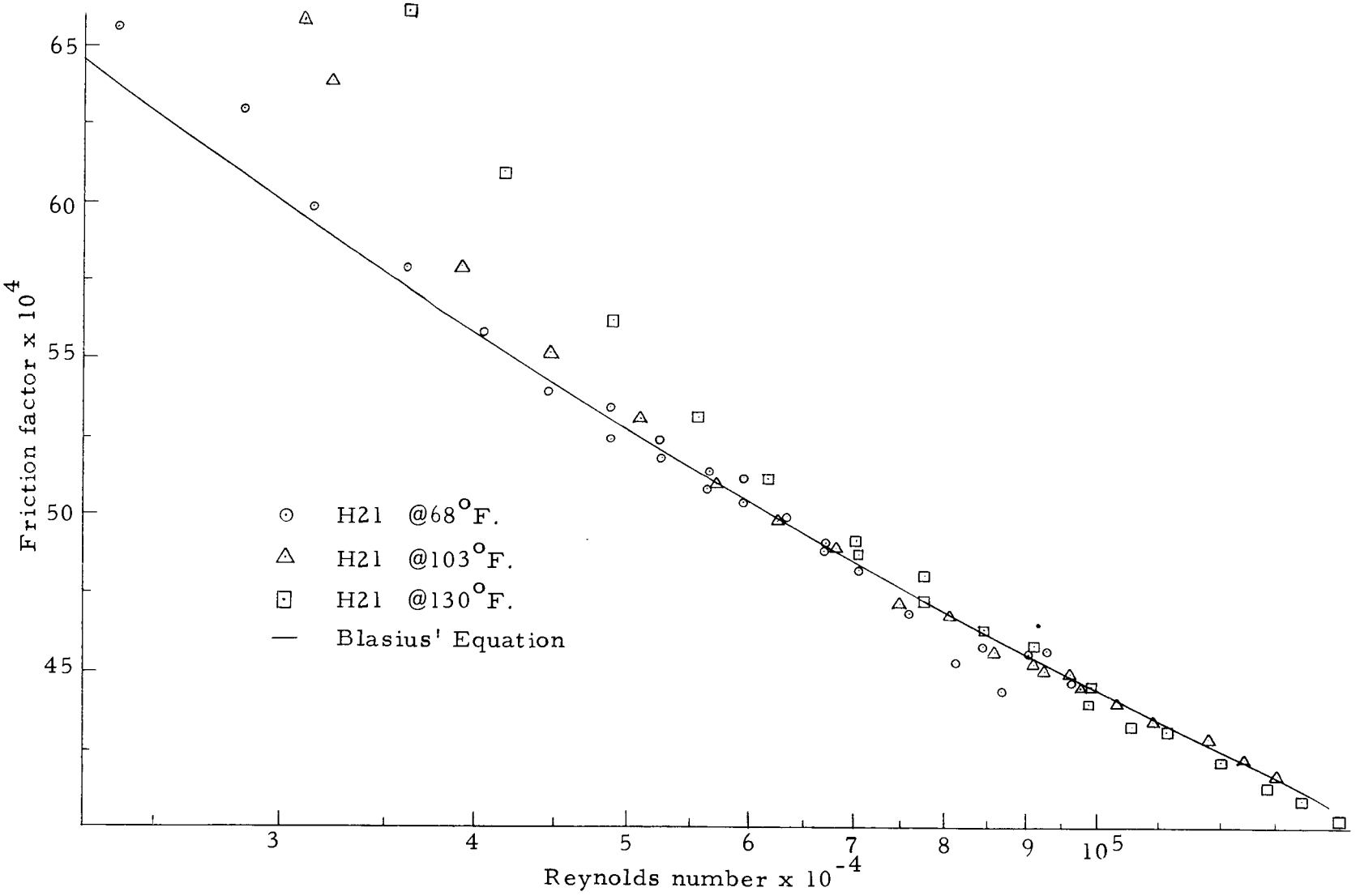

Figure 8. Friction Factor Plot of H21 @Three Temperatures

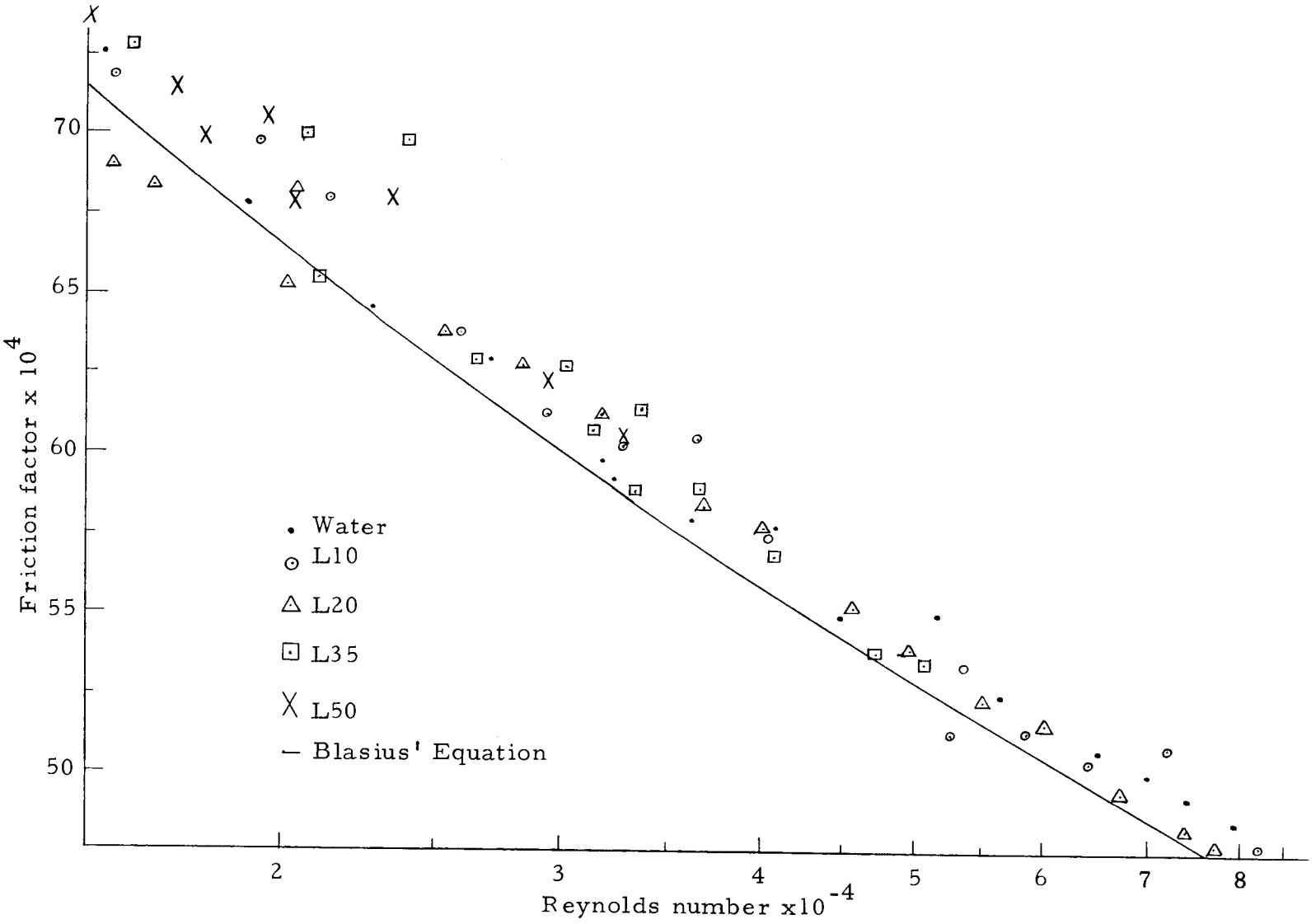

Figure 9. Ward's Friction Factor Data - Light Oil

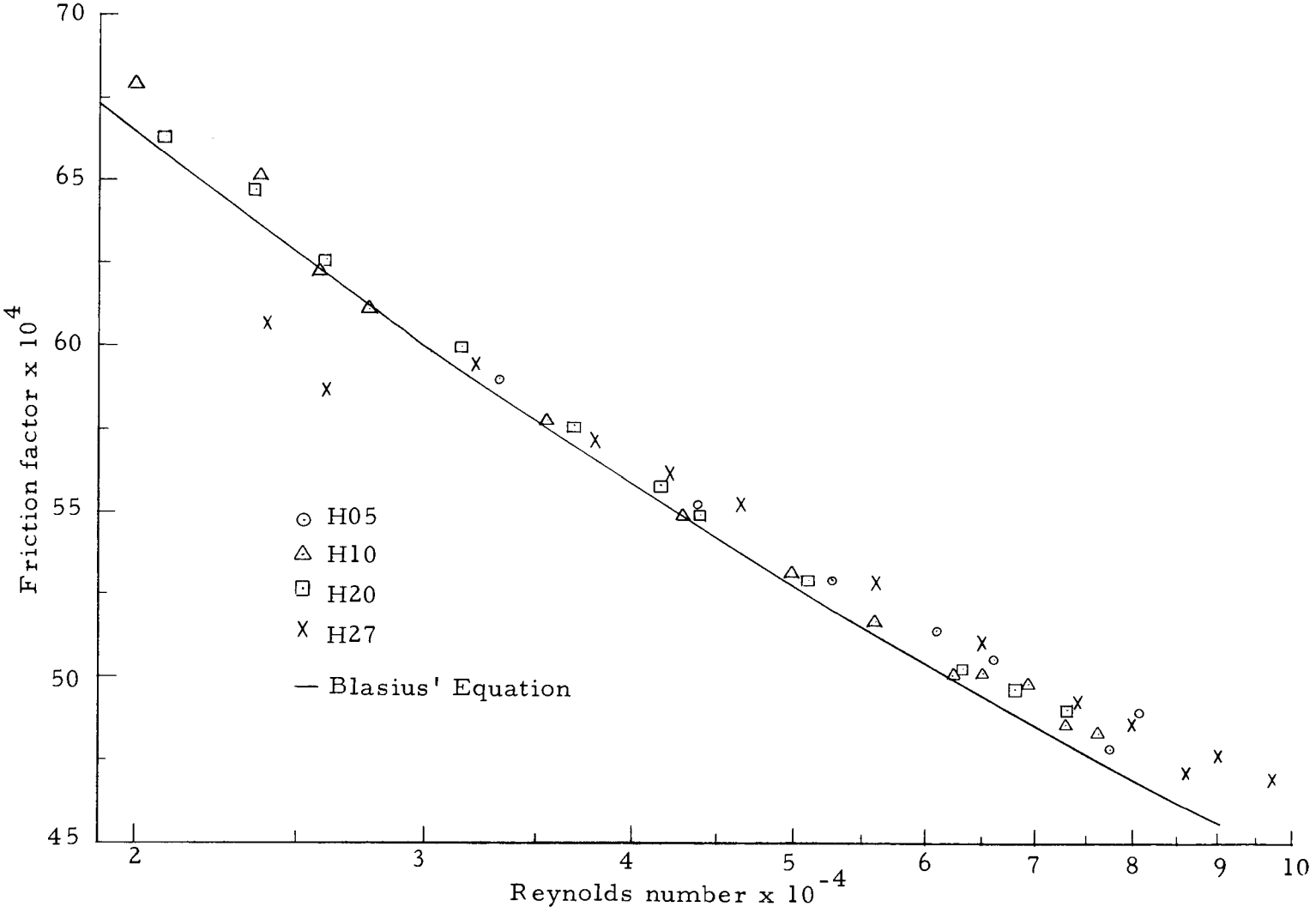

Figure 10. Ward's Friction Factor Data - Heavy Oils

The resistance to flow, as indicated by the friction factor, is seen to increase for the light oil dispersion with increasing dispersed phase concentration. This would be expected from theories on the viscosity of dispersions. Dimensionless velocity profiles obtained by Ward (22) for the light oil dispersions showed no apparent effect of flow rate except for the 50 percent dispersion at low flow rates. He, therefore, concluded that the light oil dispersions behaved as single-phase Newtonian fluids. Ward's friction factor results for HO5, H10, and H20 gave identical viscosities. These results indicate that the addition of more dispersed phase liquid did not change the effective viscosity of the dispersion, a result that is contrary to all the proposed theories and observed data on the viscosity of suspensions. This fact was confirmed in the present study. An effective viscosity for the dispersion H4.5 was 1.22 centipoises while dispersion H21 had an effective viscosity of 1.17 centipoises at 68°F. This unusual behavior was explained by Ward by examining the dropsize and dropsize distributions for the heavy oil dispersions. These distributions were characterized by a large number of drops occurring in the diameter range of 1/2 to 10 microns but the remaining drops, accounting for most of the volume, having diameters as large as 300 and in some cases 600 microns. A dropsize distribution on run H10 showed that 70 percent of the droplets occur in the diameter range of 0 to 14 microns with another 12 percent in the range 14 to 28

microns. These two intervals, however, accounted for only 0.3 percent of the total volume of the dispersed phase. On the other hand, about five percent of the droplets occur in the diameter range from 100 microns to the maximum of 300 microns. But these droplets accounted for approximately 85 percent of the dispersed phase volume. Thus one could consider this a multiple dispersion of a few large droplets dispersed in a finer near-emulsion of very small droplets. Thus, Ward concluded that the viscosity of the heavy oil dispersions would be governed by the small drops which were present.

The relative fluidity, μ_w/μ_e, of the dispersions as a function of the dispersed phase concentration is shown on Figure 11. The work of Cengel, et al., Faruqui, Ward and this work are also presented and compared in Table 8. The advantages to this method of presentation instead of the usual relative viscosity, μ_e/μ_w, are two fold: The relative fluidity-concentration curves remain linear over a much larger range and the range of the dependent variable is restricted from zero to one. This gives a definite intercept on the concentration axis when the effective viscosity approaches infinity.

Except for the data taken at room temperature, the bulk temperature of the dispersion is marked by the data point on Figure 11. A curve describing both the light oil and solvent dispersions at room temperature would exhibit a steep slope in the range zero to five volume percent. The absolute value of the slope as the concentration

approaches zero is greater than the value of 2.5 predicted by Einstein (22, p. 2). These results agree with several investigators (22, p. 136) who have concluded that the value of 2.5 for the limiting slope does not apply to polydisperse systems. The relative fluidity of the light oil dispersions is approximately linear for each bulk dispersion temperature over the range 10 to 50 volume percent. The relative fluidity of the 10, 20, and 35 volume percent solvent dispersions is also linear but the value at 50 volume percent is higher (i.e., the effective viscosity is lower) than the linear relation would predict. None of the equations presented by Ward (22, p. 23) represented the effective viscosities of the dispersions over the entire range of concentrations. Some of the equations could be made to fit the experimental data over limited concentration intervals. An example is the equation

$$(0.9)\,\mu = \mu_c e^{2.5\phi}$$

where $(0.025 < \phi < 0.50)$

which represents the effective viscosities of the light oil dispersions at 68°F. within 11.4%; the light oil dispersions at 108°F. within 9.5%; the light oil dispersions at 140°F. within 16.4%; and the petroleum solvent within 4.5%. The heavy oil dispersions at 68°F. below 10 volume percent have an average deviation of 4.3%. This equation has been included in Figure 11 as a line. Table 8 shows excellent agreement between effective viscosities determined by the method discussed in this report and the methods of previous workers.

Best scan available.

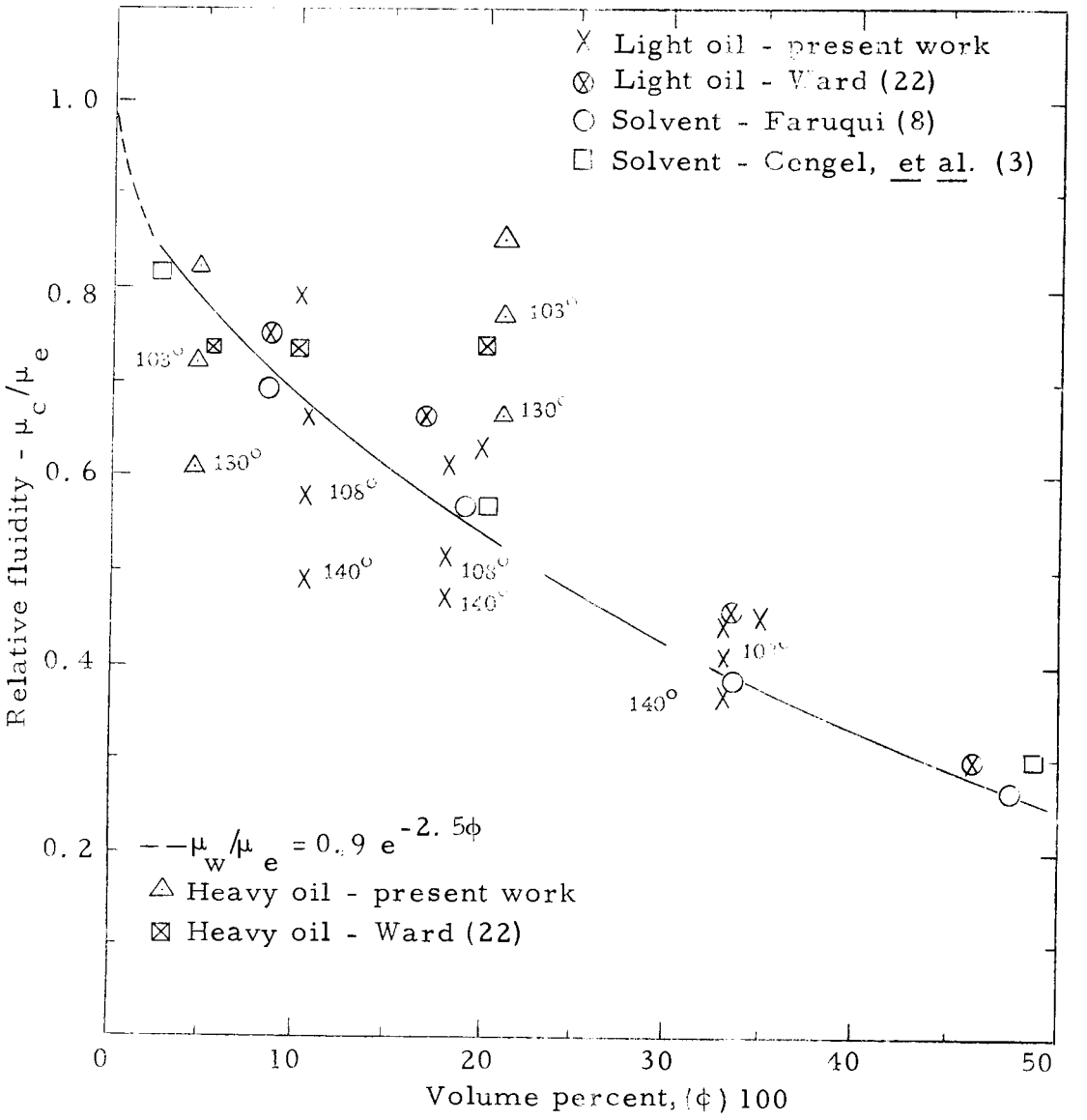

Figure 11. Relative Fluidities

Table 8. Effective Viscosities at Room Temperature in Turbulent Range of Previous Workers Compared with Pressure Drop Method

Dispersion	Cengel &Wright	Finnigan		Faruqui		Ward		Legan
		1	2	1	2	1	2	
S05	1.12							
S10				1.38	1.42			
S20	1.43	2.37	2.30/* 1.85	1.69	1.71			
S25		2.13	1.83					
S35	2.64			2.50	2.53			
S50	5-8	3.16	3.29	3.53	3.40			
S65		4.77	4.08					
L10						1.33	1.35	1.26
L20						1.51	1.49	1.57
L35						2.17	2.27	2.23
L50						3.34	3.31	
H05						1.36	1.37	1.22
H10						1.36	1.33	
H20						1.36	1.33	1.17
H27						?	1.13	

1 The viscosity reported by the author

2 The viscosity obtained by the method discussed in this thesis

* The first number is the complete set of data, the second is high flows only

As the temperature increases the relative fluidity decreases at constant concentration, a phenomenon which was unexpected. This can not be explained with existing knowledge of the physical properties of the oils or their dispersions. It is hypothesized that the oil properties, specifically viscosity and interfacial tension, exert a larger effect on the dispersion as the fluid temperature increases. It is known that the viscosity ratio of the two phases (μ_{oil}/μ_{water}) decreases rapidly with increasing temperature. However no systematic relation using this viscosity ratio as a parameter was obtainable. Interfacial tension changes slowly with temperature and therefore would not be expected to exert an appreciable effect. Higher temperatures may have caused more impurities to accumulate at the surface of the two phases and thereby cause a higher effective viscosity than was measured at room temperature.

Heat Transfer

The main purpose of taking friction factor data at higher than $68^{\circ}F$. was for the explicit reason of correlating the heat transfer data to Colburn's equation, equation (25). Previous workers in correlating their data used the viscosity of the dispersion calculated from friction factor data or velocity profiles obtained at room temperature but neglected to correct this viscosity to the film temperature. Faruqui (8) concluded from temperature profile data that the

liquid-liquid dispersions heat transfer coefficients could be predicted from existing single-phase correlations if the Prandtl number of the continuous phase at the film temperature was used. However, the effective viscosity of the dispersion at the film temperature was not used to calculate the Reynolds number.

Friction factor data were taken at 108°F. and 140°F. because these temperatures bounded the film temperature for the water run. Thus the effective viscosity of the dispersion at their film temperatures were obtained by interpolation as shown in the Sample Calculation section.

The heat transfer results for the light and heavy oil dispersions are compared with Colburn's equation in Figures 12 and 13. A sharp deviation from Colburn's equation is seen for the light oil dispersions at low flow rates. The deviation increases as the Reynolds number decreases. Run L30 has lower heat transfer coefficients than water, H 4.5, or H21 at the low flow rates as shown on Figure 15. Figure 13 shows that the heavy oil dispersions can be predicted by Colburn's equation over the complete range of Reynolds number, especially at the low flow rates. Ward's heavy oil velocity profiles showed an apparent flow rate dependency. Velocity profiles determined at a low and a high flow rate for the dispersion H10 were examined and compared. The low flow rate velocity profile could predict an effective viscosity of 1.36 centipoise, exactly the value obtained by

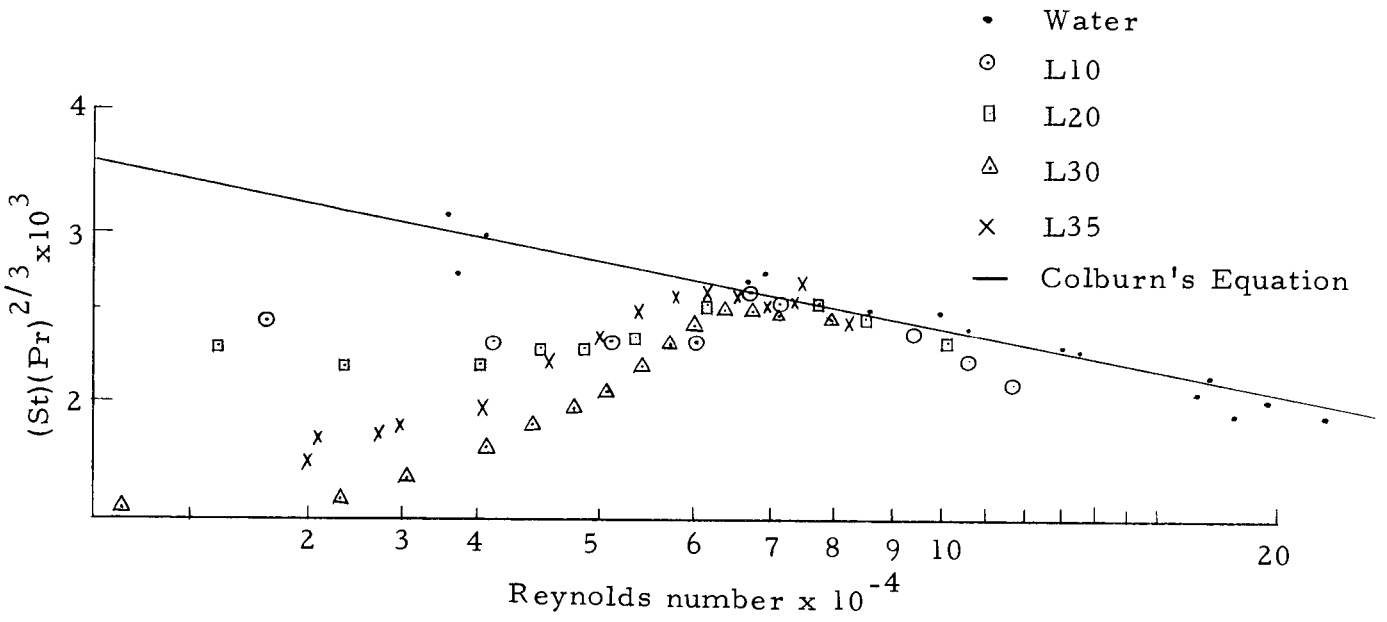

Figure 12. Light Oil Heat Transfer Results

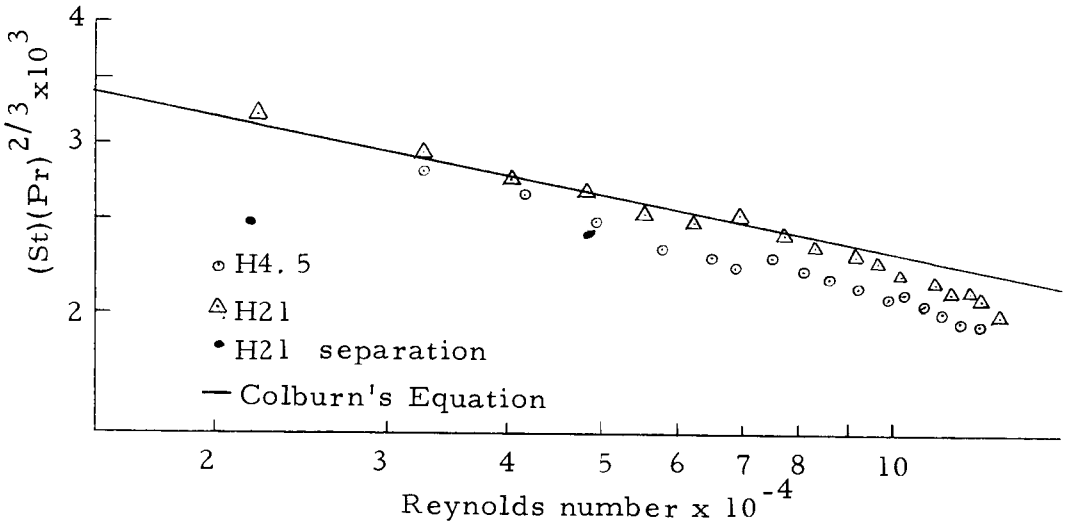

Figure 13. Heavy Oil Heat Transfer Results

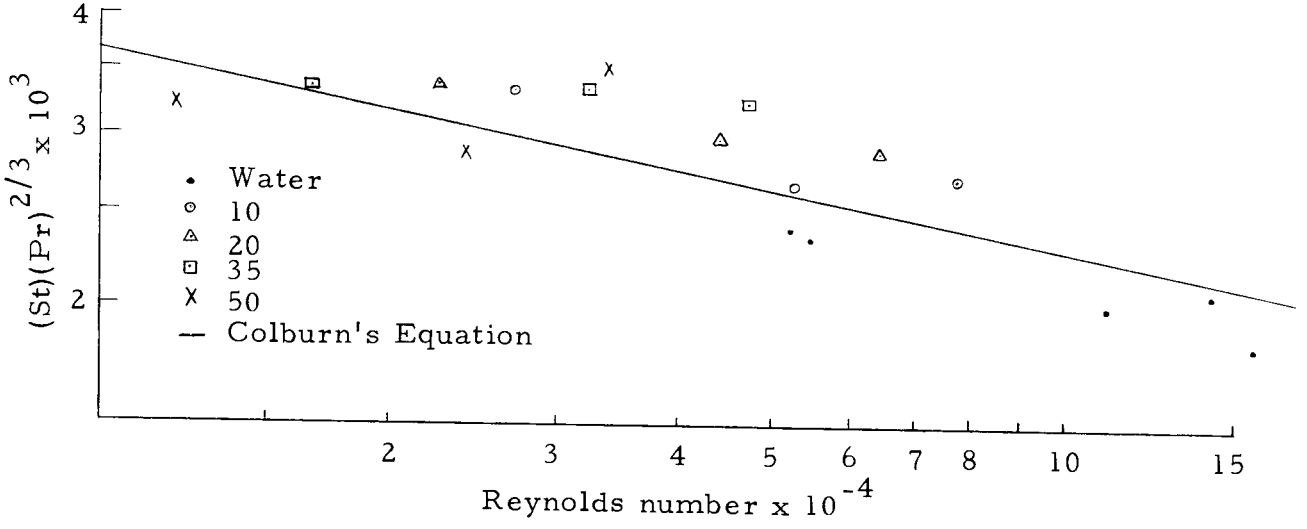

Figure 14. Faruqui's Heat Transfer Results

matching the experimental and accepted friction factor curves. However, the high flow rate velocity profile predicted an effective viscosity of 1.1 centipoises which was much too low to account for the observed friction factor data. This observation agrees with the heat transfer results which deviate from Colburn's equation at the higher flow rates. This seemingly confusing fact that the light oil dispersions deviated from Colburn's equation by a large amount at the low flow rates while the heavy oil dispersions did not will be explained by the assumption that the light oil dispersions separate as the film temperature increases resulting in a film that does not consist of the complete continuous phase.

To check the apparatus and procedure, heat transfer results were obtained for water and compared with Colburn's equation, Figure 12. Close agreement is seen to exist even at the lower flow rates. Figure 12 also shows that the light oil dispersions agree well with Colburn's equation above a Reynolds number of 50,000. Table 9 gives a least square slope, y-intercept, and the y-intercept if the data were fitted to Colburn's slope, -0.2, for the light and heavy oil dispersions. The complete range of data is included along with a least squares analysis of only the data above a Reynolds number of 50,000. By analyzing only the high flow rates the Colburn's y-intercept, 0.023, was obtained for all light and heavy oil dispersions except for run H4.5 which had a y-intercept of 0.021. The light oil

Table 9. Summary of Heat Transfer Results[1]

Run	Slope	Y-intercept	Y-intercept fitted to a slope of (-. 2)
Water	-0. 214 ± . 015	0. 027 ± . 005	0. 023
L10	-0. 043 ± . 034	0. 0037 ± . 0014	0. 021
L20	0. 063 ± . 029	0. 0012 ± . 0004	0. 020
L30	0. 341 ± . 033	0. 00005	0. 018
L35	0. 286 ± . 031	0. 0001	0. 020
H4. 5	-0. 272 ± . 011	0. 047 ± . 006	0. 021
H21	-0. 259 ± . 010	0. 044 ± . 005	0. 023
	Neglecting flows below 50, 000 Re		
L10	-0. 172 ± . 090	0. 016 ± . 019	0. 023
L20	-0. 202 ± . 057	0. 023 ± 0. 016	0. 023
L30	-0. 176 ± . 048	0. 017 ± . 010	0. 023
L35	-0. 172 ± . 065	0. 017 ± . 013	0. 023
Combined light oil	- . 206 ± 0. 035	0. 024 ± . 010	0. 023
H4. 5	-0. 246 ± . 020	0. 035 ± . 008	0. 021
H21	-0. 239 ± 0. 010	0. 035 ± . 004	0. 023
	Faruqui's Results (8)		
Water	-0. 202 ± . 045	0. 022 ± . 012	0. 021
10	-0. 212 ± . 091	0. 029 ± . 033	0. 025
20	-0. 156 ± 0. 027	0. 016 ± . 005	0. 026
35	-0. 023 ± . 020	0. 004 ± . 001	0. 026
50	0. 057 ± . 190	0. 002 ± . 006	0. 024

[1] Data fitted to $(St)Pr^{2/3} = 0.023\ Re^{-.2}$

dispersions yielded slopes from -0.17 to -0.20 which are very close to Colburn's slope, -0.20. The heavy oil dispersions had steeper slopes of approximately -0.26 over the complete range of Reynolds number. A maximum 10 percent deviation from Colburn's equation was observed at high flow rates for the heavy oil dispersions, while the light oil dispersions were low by a factor of two at the low flow rates. This large deviation was believed to be caused by the light oil dispersions separating at the higher film temperatures. It was observed in the experimental work that the light oil dispersions samples taken to determine the dispersions concentration separated more easily than did the heavy oil dispersions. This may link the heat transfer results for the light and heavy oil dispersions at the low flow rates. Therefore, it was assumed that the light oil dispersions separate at high film temperatures and the heavy oil dispersions did not have a tendency to separate at the existing film temperatures. To substantiate these assumptions heat transfer data for run H21 were taken at a bulk temperature of 130°F. If these results deviated from Colburn's equation as did the light oil then the assumption could be concluded to be correct because the heavy oil dispersions separated readily at the higher bulk fluid temperatures. Two flow rate settings were chosen to confirm the assumptions: 0.48 and 1.2 pounds/second. The corresponding film temperatures were 185°F. and 164°F. The results shown on Figure 13 as black circles did deviate from the

previous results in the same manner as the light oil dispersions. For instance, at 0.48 pounds/second $(St)(Pr)^{2/3}$ decreased from 0.0032 to 0.0025, a 22 percent deviation. An examination of Figure 15 shows the heat transfer coefficients for the light oil dispersions are lower than either water or the heavy oil dispersions at the low flow rates. Also Figures 3 through 8 indicate the friction factors at the higher temperatures ($108^{\circ}F.$ and $140^{\circ}F.$) increase rapidly giving friction factors much higher than predicted at the low flow rates as the bulk fluid temperature increases. Considering the above factors it is concluded that the two assumptions as stated above are true.

Faruqui's heat transfer results are shown on Figure 14 for comparison. A least square analysis of this data is listed in Table 9. Since neither the petroleum solvent which Faruqui used or the heavy oil dispersions in the present work showed deviation from Colburn's equation at the low flow rates this separation tendency of the light oil dispersions must be a characteristic of the light oil dispersions. The heat transfer coefficients, in general, can be predicted from Colburn's equation; however, the liquid-liquid dispersion as in the case of the light oil dispersion may exhibit separation properties that will yield lower heat transfer coefficients.

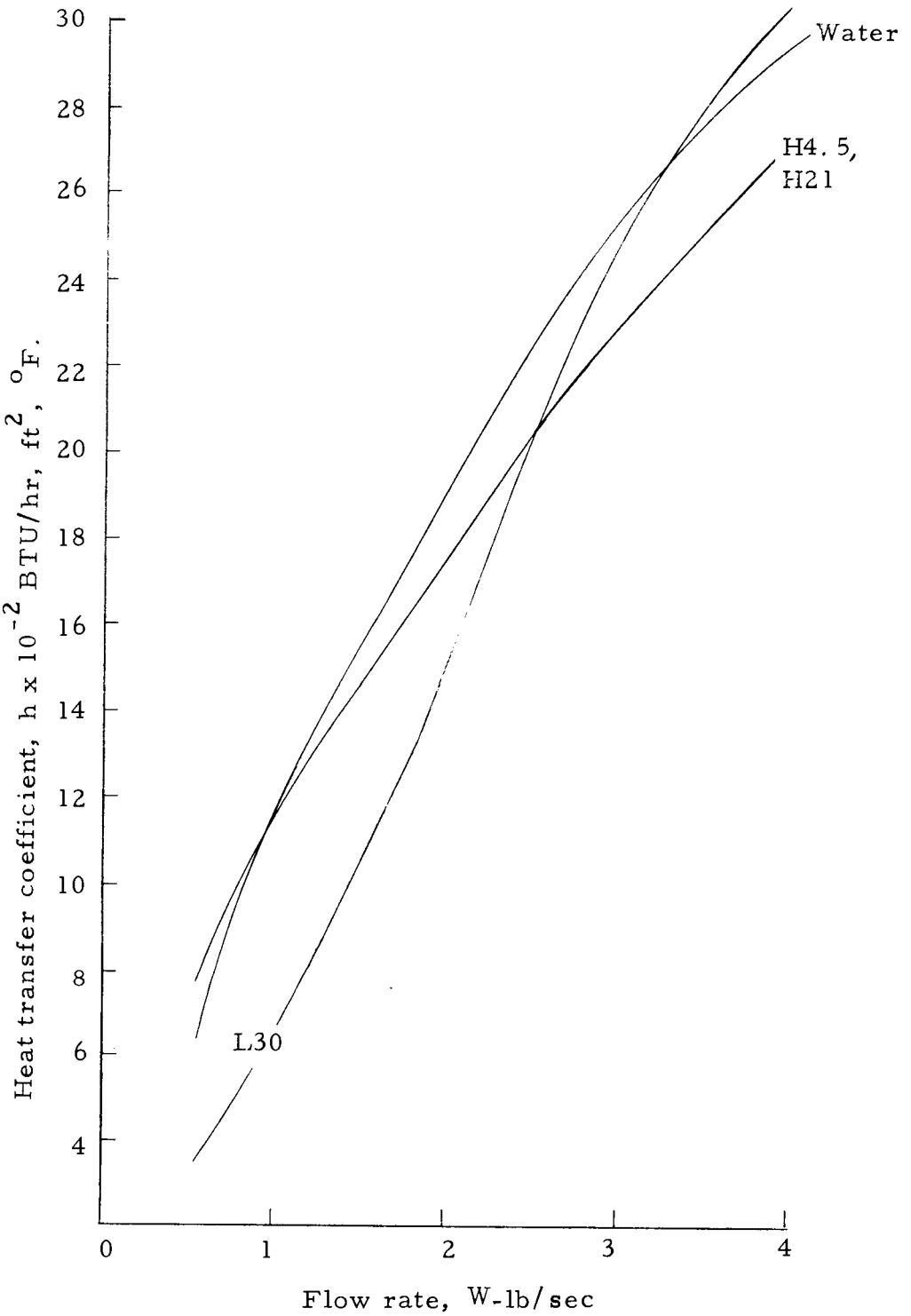

Figure 15. Variation of Heat Transfer Coefficients with Flow Rate

CONCLUSIONS

The friction losses of liquid-liquid dispersions investigated in this report can be treated with existing single-phase equations. By fitting the friction factors to Blasius' equation an effective viscosity of the liquid-liquid dispersion can be obtained that agrees with a viscosity obtained by analyzing velocity profiles. The procedure used appears to be superior to previous methods because of less scatter of the data.

The effective viscosity of the heavy oil dispersions indicate that the addition of more dispersed phase liquid does not change the effective viscosity of the dispersions. This unusual behavior is explained by a "slip" velocity of the large drop relative to a fluid element in which they are contained.

The relative fluidity of the petroleum solvent (investigated by Faruqui), the light oil, and the heavy oil dispersion below 10 volume percent in water can be represented between 4 and 16 percent by $0.9\,\mu_e = \mu_c e^{2.5\phi}$ in the concentration range $.025 < \phi < .50$. The relative fluidity decreases with increasing bulk dispersion temperature. The reason for this effect is not known at present and future work is warranted.

At the low flow rates and high bulk fluid temperatures, the measured friction factors were much larger than the results

obtained for the dispersion at room temperature or predicted by Blasius' equation. The effective viscosity of these dispersions was dependent upon flow rates in this region and the pressure drop due to friction was not proportional to the flow rate to the 1.75 power. This effect was because of phase separation of the liquid-liquid dispersions. It is assumed that a "slip" factor of the dispersed droplets caused higher friction factors upon the dispersions separation. Again, further experimental work is needed to explain the rapid increase in friction factors at low flow rates.

The heat transfer coefficient for liquid-liquid dispersions, in general, can be predicted from Colburn's equation using the continuous phase Prandtl number evaluated at the film temperature and using the effective viscosity at the film temperature to calculate the Reynolds number. Separation of the light oil dispersions occurred below a Reynolds number of 50,000 causing large deviations from Colburn's equation. At these high film temperatures the film was apparently not a continuous phase but a mode of both phases present. Below one pound/second runs L30 and L35 could be correlated within 10 percent of Colburn's equation by using effective dispersion properties in calculating the Prandtl number.

RECOMMENDATIONS

Further Work

Friction factors, heat transfer coefficients, and velocity and temperature profiles of liquid-liquid dispersions should be further investigated. It is suggested that a complete study of the oils in this investigation, as well as others, be made to investigate the effects their physical properties have on the dispersion as the temperature is increased. This study should include a complete range of dispersed phase concentration. Dispersions where the oil is the continuous phase have been studied only slightly and merit further investigation. Continued research may be able to determine which properties of the dispersion determine the continuous phase, at what concentration, and why the discontinuous phase becomes the continuous phase.

The procedure for analyzing pressure drop data to obtain effective viscosities of a liquid-liquid dispersion as presented in this work needs further comparison with velocity profiles obtained above room temperature. No previous work appears to have been done. This work should also investigate the effect of temperature on friction factors, velocity profiles, dropsize, and dropsize distribution. Especially needed in correlating the heat transfer studies are

temperature effects on the wall film and the Prandtl number. The region of mass flows below Reynolds number of 50,000 merit special study because of the apparent separation effect present in this region.

Apparatus Design Changes

To reduce experimental error some design changes are recommended. A method to determine accurately the wall temperature of the test section needs to be devised. Thermocouples installed in the same thermocouple well give temperature differences of up to 15°F. These large temperature differences contributed a 4% error in the heat transfer data. To keep the dispersions from separating at the high temperatures a mixer designed for this purpose installed at the beginning of the test section may eliminate some of the experimental error contributed to the separation of the dispersion. A one percent error in the pressure drop could easily be reduced by using lighter manometer fluids. Extending the manometers to six feet in length and using 1.2 and 2.94 specific gravity manometer fluids should eliminate this error.

BIBLIOGRAPHY

1. Baron, Thomas, C.S. Sterling and A.P. Schueler. Viscosity of suspensions--Review and application to two phase flow. Midwestern Conference on Fluid Mechanics, Proceedings 3:103-123. 1953.

2. Blasius, H. Das Aehnlichkeitsgesetz bei Reibungsvosgangen in Flussigkeiten. VDI Forschungsarben 131:1-40. 1913.

3. Cengel, John A. et al. Laminar and turbulent flow of liquid-liquid emulsions. Journal of the American Institute of Chemical Engineers 8:335-339. 1962.

4. Cengel, John A. Viscosity of liquid-liquid dispersions in laminar and turbulent flow. Master's thesis. Corvallis, Oregon State College, 1959. 110 numb. leaves.

5. Colburn, Allan P. A method of correlating forced convection heat transfer data and a comparison with fluid friction. Transactions of the American Institute of Chemical Engineers 29:174-208. 1933.

6. Dodge, D.W. and A.B. Metzner. Turbulent flow of non-Newtonian systems. Journal of the American Institute of Chemical Engineers 5:189-204. 1959.

7. Drew, T.B., E.C. Koo and W.H. McAdams. The friction factor for clean sound pipes. Transactions, American Institute of Chemical Engineers 28:56. 1932.

8. Faruqui, Azimuddin A. Velocity and temperature profiles for turbulent flow of liquid-liquid dispersions in pipes. Ph.D. thesis. Corvallis, Oregon State University, 1962. 134 numb. leaves.

9. Faruqui, A.A. and James G. Knudsen. Velocity and temperature profiles of unstable liquid-liquid dispersions in vertical turbulent flow. Chemical Engineering Science 17:897. 1962.

10. Finnigan, Jerome W. Pressure losses and heat transfer for the flow of mixtures of immiscible liquids in circular tubes. Ph.D. thesis. Corvallis, Oregon State College, 1958. 154 numb. leaves.

11. Hadamard, J. Mouvement permanent lent d'une sphere liquide et visqueuse dans un liquide visquex. Academic des sciences, Paris. Comptes Rendus 152:1735-1738. 1911.

12. Karman, T. von. Mechanical similitude and turbulence. Washington, National Advisory Committee on Aeronautics, March 1931. 19 p. (Technical momo no. 611)

13. Knudsen, James G. and Donald L. Katz. Fluid dynamics and heat transfer. New York, McGraw-Hill, 1958. 576 p.

14. Maude, A. D. and R. L. Whitmore. The turbulent flow of suspensions in tubes. Transactions of the Institute of Chemical Engineers 36:296-304. 1958.

15. Metzner, A. B. and P. S. Friend. Heat transfer to turbulent non-Newtonian fluids. Industrial and Engineering Chemistry 51:879-882. 1959.

16. Mohun, W. A. and W. S. Peterson. Precision of heat transfer measurements with thermocouples-- Geometric errors. Canadian Chemistry and Process Industries. Oct. 1947, 908-913 p.

17. Nikuradse, J. Gesetzmaessigkeiten des turbulenten stroemung in glatten rohren. Forschungsheft 3:356. 1932.

18. Orr, Clyde, Jr. and J. M. Dallavalle. Heat transfer properties of liquid-solid suspensions. In: Heat Transfer--Research studies for 1954. Chemical Engineering Progress Symposium, ser. 9, 50:29-45. 1954.

19. Reynolds, Osborne, An experimental investigation of the circumstances which determine whether the motion of water shall be direct or sinuous, and of the law of resistance in parallel channels. Philosophical Transactions of the Royal Society (London) A174:935. 1884.

20. Shaver, Robert G. and Edward W. Merrill. Turbulent flow of pseudoplastic polymer solutions in straight cylinderical tubes. American Institute of Chemical Engineers, Journal 2:181-188. 1959.

21. Stanton, T. E. and J. R. Pannell. Similarity of motion in relation to the surface friction of fluids. Philosophical Transactions of the Royal Society (London) A214:199. 1914.

22. Ward, John P. Turbulent flow of liquid-liquid dispersions: Drop size, friction loss, and velocity distributions. Ph. D. thesis. Corvallis, Oregon State University, 1964. 353 numb. leaves.

23. Wright, Charles H. Pressure drop and heat transfer for liquid-liquid dispersions in turbulent flow in a circular tube. Master's thesis. Corvallis, Oregon State College, 1957. 120 numb. leaves.

APPENDIX

TABLE 10

OBSERVED AND CALCULATED FRICTION FACTOR DATA

W lb_m/sec.	HT cm	$-\Delta P_f$ lb_f/ft^2	f x 10^4	RE175
	Water at 72° F.			
4.115	18.3	469.284	43.28	116340
4.127	18.6	476.977	43.78	116679
3.376	82.5	324.152	44.40	95446
3.376	79.0	328.242	44.97	95446
3.274	12.2	310.400	45.27	92563
3.274	79.0	312.856	45.63	92563
3.010	67.4	264.668	45.63	85099
3.010	10.4	266.676	45.98	85099
2.998	67.6	265.608	46.19	84760
2.998	10.4	266.697	46.38	84760
2.501	48.6	190.893	47.68	70708
2.012	33.8	132.726	51.25	56883
1.492	19.9	78.143	54.87	43889
1.035	10.5	41.231	60.17	30445
0.884	7.8	30.629	61.27	26004
0.493	2.8	10.995	70.72	14501
	Run L10 at 68°F.			
4.055	19.5	494.961	46.37	88850
3.619	16.0	405.125	47.65	79297
3.106	12.2	307.588	49.11	68056
3.106	78.9	306.677	48.97	68056
2.731	9.7	243.419	50.27	59839
2.731	62.6	242.173	50.02	59839
2.320	7.4	184.384	52.77	50834
2.320	47.6	182.813	52.32	50834
1.950	35.2	133.742	54.18	42727
1.950	5.5	135.615	54.94	42727
1.534	24.0	89.364	58.50	33611
1.157	15.6	56.142	64.60	25350
0.780	8.3	27.270	69.05	17090
	Run L10.4 at 68°F.			
4.042	20.3	515.693	48.65	74465
3.861	18.7	474.625	49.07	71131
3.662	17.0	430.990	49.53	67465
3.500	15.6	395.056	49.70	64480
3.331	14.2	359.121	49.88	61367
2.941	11.5	289.819	51.64	54182
2.941	74.1	287.880	51.30	54182
2.750	66.1	256.221	52.22	50663
2.750	10.3	259.018	52.79	50663
2.548	09.0	225.650	53.57	46941
2.548	58.1	224.563	53.31	46941
2.369	51.7	199.236	54.71	43644
2.369	8.0	199.982	54.92	43644
2.190	7.0	174.315	56.02	40346

(1) (continued)

W lb_m/sec.	HT cm	$-\Delta P_f$ lb_f/ft^2	f x 10^4	RE175
	Run L10.4 (continued)			
2.190	45.2	173.513	55.76	40346
2.025	39.3	150.165	56.44	37306
2.025	06.1	151.214	56.83	37306
1.838	5.2	128.113	58.45	33861
1.838	33.4	126.817	57.86	33861
1.618	26.8	100.698	59.28	29808
1.422	21.9	81.307	61.97	26197
1.218	17.1	62.312	64.74	22439
1.043	13.1	46.483	65.86	19215
.795	9.0	30.258	73.79	14645
	Run L10.4 at 108°			
4.055	18.8	476.756	44.33	104100
3.867	17.2	435.672	44.55	99274
3.772	16.5	417.647	44.88	96835
3.592	15.1	381.732	45.24	92214
3.447	14.2	358.676	46.16	88491
3.327	13.3	335.586	46.36	85411
3.107	11.8	297.101	47.06	79763
3.013	11.2	281.708	47.45	77350
3.103	72.5	280.267	47.21	77350
2.826	64.5	248.719	47.62	72549
2.826	10.0	250.920	48.04	72549
2.632	57.1	219.537	48.46	67569
2.632	8.9	222.699	49.16	67569
2.427	7.8	194.464	50.48	62306
2.427	49.9	191.061	49.60	62306
2.233	43.2	164.650	50.49	57325
2.233	6.7	166.244	50.98	57325
2.043	5.9	145.721	53.38	52448
2.043	37.4	141.787	51.94	52448
1.828	30.9	116.134	53.14	46928
1.643	26.2	97.612	55.29	42179
1.426	21.0	77.119	57.99	36609
1.266	17.4	62.932	60.04	32501
1.062	13.4	47.168	63.95	27264
.788	8.8	29.040	71.51	20230
	Run L10.4 at 140°F.			
4.023	18.1	458.669	42.97	117645
3.895	17.1	433.013	43.28	113902
3.754	16.0	404.754	43.55	109779
3.625	15.0	379.086	43.74	106006
3.493	14.1	355.998	44.24	102146
3.313	12.9	325.202	44.92	96883
3.182	11.9	299.550	44.86	93052
3.182	76.8	296.781	44.44	93052

(continued)

TABLE 10 (continued)

W $lb_m/sec.$	HT cm	$-\Delta P_f$ lb_f/ft^2	$f \times 10^4$	RE175
	Run L10.4 at 140°F. (continued)			
2.978	68.7	264.878	45.29	87086
2.987	10.6	266.203	45.51	87086
2.765	9.4	235.421	46.69	80857
2.765	60.4	232.187	46.05	80857
2.593	56.4	216.433	48.81	75827
2.593	8.4	209.769	47.30	75827
2.416	7.6	189.247	49.16	70651
2.416	48.6	185.711	48.24	70651
2.242	43.1	164.049	49.48	65563
2.242	6.7	166.161	50.12	65563
2.050	5.7	140.509	50.69	59948
2.078	37.5	141.992	49.86	60767
1.848	31.3	117.573	52.20	54041
1.670	26.3	97.880	53.21	48836
1.509	22.7	83.701	55.73	44126
1.304	18.2	65.977	58.83	38132
1.100	13.9	49.041	61.43	32167
.836	10.1	34.074	73.93	24447
	Run L18 at 70°F.			
4.014	20.6	519.446	49.14	68637
3.796	18.6	468.110	49.52	64909
3.553	16.6	416.775	50.33	60754
3.340	14.9	373.140	50.99	57112
3.179	13.7	342.339	51.64	54359
2.849	11.4	283.304	53.21	48716
2.849	73.8	282.745	53.10	48716
2.658	65.5	249.899	53.92	45450
2.658	10.2	252.503	54.48	45450
2.467	9.0	221.702	55.53	42183
2.467	58.1	220.615	55.26	42183
2.256	50.1	188.956	56.60	38575
2.256	7.8	190.901	57.18	38575
2.370	54.5	206.887	56.15	40525
2.370	8.4	206.367	56.01	40525
2.014	41.6	155.619	58.49	34437
1.811	35.2	130.246	60.54	30966
1.629	29.6	108.044	62.07	27854
1.370	22.7	80.689	65.54	23426
1.082	16.1	54.523	71.0	18501
1.234	19.4	67.606	67.68	21100
.850	11.6	36.682	77.40	14533
..737	9.6	28.753	80.70	12602
1.811	5.5	131.898	61.31	30966
2.014	6.6	160.138	60.18	34437
	Run L18 at 108°F			
3.996	19.2	482.985	45.73	91386
3.776	17.4	436.791	46.32	86354
3.541	15.5	388.030	46.79	80980
3.279	13.5	336.703	47.35	74988
2.994	11.7	290.508	49.00	68470
2.994	75.3	287.885	48.56	68470
2.800	67.4	256.658	49.50	64034
2.800	10.5	259.712	50.08	64034
2.569	58.6	221.874	50.83	58751
2.569	9.1	223.783	51.27	58751
2.384	8.1	198.119	52.70	54520
2.384	52.0	195.786	52.08	54520
2.200	44.4	165.745	51.78	50312
2.200	6.9	167.323	52.27	50312
2.018	6.0	144.225	53.55	46150
2.018	38.6	142.819	53.02	46150
1.800	32.8	119.893	55.95	41164
1.654	28.3	102.106	56.43	37825
1.439	22.8	80.366	58.68	32909
1.261	19.0	65.346	62.13	28836
1.078	15.2	50.325	65.48	24651
.860	11.5	35.700	72.98	19666
	Run L18 at 140°F.			
3.985	18.4	462.298	43.63	110997
3.512	14.8	369.887	44.95	97822
3.272	13.1	326.266	45.68	91137
3.026	11.4	282.644	46.26	84285
3.026	73.8	281.497	46.08	84285
2.836	66.1	251.096	46.79	78993
2.836	10.2	251.849	46.93	78993
2.628	9.0	221.058	47.97	73197
2.628	58.0	219.116	47.55	73197
2.435	52.1	195.685	49.47	67822
2.435	8.1	197.951	50.04	67822
2.280	7.3	177.425	51.15	63505
2.280	46.9	175.169	50.50	63505
2.113	41.2	152.679	51.25	58853
2.113	6.4	154.333	51.81	58853
1.901	35.1	128.542	53.31	52948
1.682	29.1	104.881	55.56	46849
1.474	23.9	84.335	58.18	41055
1.253	19.0	65.020	62.07	34899
.985	14.1	45.705	70.61	27434
.756	10.3	30.725	80.58	21057
3.767	15.8	395.547	41.78	104922

TABLE 10 (continued)

W lb_m/sec.	HT cm	$-\Delta P_f$ lb_f/ft^2	f x 10^4	RE175	W lb_m/sec.	HT cm	$-\Delta P_f$ lb_f/ft^2	f x 10^4	RE175
	Run L20 at 68°F.					Run L33 at 180°F.			
4.004	20.2	508.941	48.39	70397	3.898	20.6	510.501	49.66	70532
3.736	17.8	447.358	48.85	65685	3.884	20.0	495.111	48.51	70278
3.524	16.1	403.737	49.55	61957	3.679	18.2	448.941	49.03	66569
3.233	13.9	347.285	50.64	56841	3.422	16.2	397.641	50.19	61919
3.071	12.9	321.626	51.98	53993	3.219	15.2	371.991	50.76	59548
2.940	11.9	295.942	52.19	51690	3.173	14.2	346.341	50.85	57413
2.940	76.8	293.632	51.78	51690	2.895	12.0	289.912	51.13	52383
2.714	10.4	257.456	53.28	47716	2.775	11.2	269.392	51.71	50212
2.714	67.4	256.544	53.09	47716	2.775	72.0	265.530	50.97	50212
2.446	57.7	218.140	55.57	43004	2.730	71.5	264.262	52.41	49397
2.174	47.7	178.708	57.63	38222	2.730	11.0	263.562	52.27	49397
1.921	5.9	141.984	58.65	33774	2.438	9.3	219.081	54.48	44114
1.921	38.2	141.247	58.34	33774	2.438	60.2	220.657	54.87	44114
1.585	28.3	102.209	62.01	27867	2.155	49.7	177.750	56.58	38993
1.432	24.3	86.436	64.25	25175	2.155	7.7	179.617	57.17	38993
1.253	20.0	69.480	67.46	22028	1.949	6.6	151.403	58.92	35266
1.085	16.3	54.890	71.07	19075	1.949	42.5	149.408	58.15	35266
.891	12.6	40.300	77.38	15663	1.701	34.7	118.704	60.64	30778
.654	8.1	22.556	80.38	11497	1.701	5.4	120.623	61.62	30778
.654	79.3	22.877	81.53	11497	1.416	25.7	83.210	61.35	25622
2.174	7.4	180.468	58.20	38222	1.268	23.1	72.929	67.04	22943
2.446	9.0	221.517	56.43	43004	1.018	17.5	50.913	72.61	18420
	Run L33 at 70°F.				.817	13.5	35.188	77.93	14783
3.912	22.0	547.283	53.32	49573		Run L32 at 140°F.			
3.748	20.2	501.106	53.21	47483	1.812	5.7	128.664	57.47	39737
3.505	18.2	449.763	54.61	44404	2.054	6.9	159.449	55.43	45044
3.265	16.0	396.447	55.47	41363	2.340	8.4	197.929	53.02	51316
3.058	14.3	349.721	55.78	38741	2.615	10.0	238.998	51.26	57347
2.765	12.1	293.287	57.22	35029	2.856	11.4	274.936	49.44	62632
2.595	10.9	262.504	58.15	32875	3.892	19.3	477.600	46.24	85352
2.595	70.4	260.180	57.63	32875	3.627	17.2	423.722	47.24	79540
2.316	59.1	218.896	60.87	29341	3.354	15.0	367.279	47.88	73553
2.316	9.2	215.673	59.98	29341	3.080	13.0	315.988	48.85	67544
2.089	7.8	182.984	62.55	26465	2.856	73.5	272.289	48.96	62632
2.089	50.2	180.619	61.74	26465	2.615	64.2	235.614	50.53	57347
1.877	42.5	152.189	64.44	23779	2.340	54.2	196.036	52.51	51316
1.877	6.6	150.194	63.59	23779	2.054	44.3	157.021	54.59	45044
1.630	5.3	118.844	66.72	20650	1.812	36.2	125.099	55.88	39737
1.630	34.3	117.916	66.20	20650	1.485	27.5	90.813	60.40	32565
1.411	27.9	93.194	69.83	17875	1.644	31.8	107.686	58.44	36053
1.411	4.3	92.723	69.47	17875	1.176	20.4	62.833	66.64	25789
1.129	20.4	63.201	73.96	14303	.962	16.2	46.281	73.35	21096
.943	16.0	45.881	76.97	11946	.900	15.3	42.734	77.38	19736
					.800	13.9	37.216	85.29	17544
					.686	11.6	28.126	87.66	15043
					.476	9.5	19.855	128.53	10438
					1.341	24.6	79.328	64.70	29408

TABLE 10 (continued)

W $lb_m/sec.$	HT cm	$-\Delta P_f$ lb_f/ft^2	$f \times 10^4$	RE175
	Run L35 at 68 °F.			
3.934	22.1	550.475	53.16	48739
3.763	20.5	509.459	53.77	46620
3.552	18.6	460.746	54.57	44006
3.360	17.0	419.690	55.55	41627
3.147	15.1	370.937	55.97	38988
2.859	12.9	314.486	57.50	35420
2.585	11.0	265.711	59.42	32026
2.585	70.6	262.030	58.60	32026
2.300	9.1	216.961	61.29	28495
2.300	58.4	213.894	60.43	28495
2.055	7.2	165.634	58.61	25459
1.812	38.7	137.412	62.54	22448
1.812	6.1	136.078	61.94	22448
1.567	4.8	106.598	64.87	19413
1.567	31.2	106.310	64.70	19413
1.265	23.0	74.026	69.13	15671
1.059	18.1	54.735	72.94	13119
	Run H4.5 at 68°F.			
4.117	19.6	501.324	46.03	93440
3.967	18.3	467.946	46.27	90035
*3.807	17.1	437.136	46.93	86401
3.680	15.9	406.294	46.67	83522
3.572	15.1	385.755	47.03	81070
3.426	14.1	360.082	47.72	77757
3.297	13.0	331.841	47.49	74829
3.095	11.7	298.465	48.47	70244
3.095	75.8	298.599	48.49	70244
*2.966	69.6	274.019	48.45	67316
2.966	10.8	275.359	48.69	67316
2.790	9.8	249.686	49.90	63322
2.790	62.9	247.456	49.45	63322
2.640	56.9	223.669	49.92	59918
2.640	8.9	226.579	50.57	59918
2.479	8.0	203.473	51.50	56263
2.479	51.2	201.071	50.90	56263
2.319	45.6	178.869	51.74	52632
*2.319	7.2	182.935	52.92	52632
*2.141	6.3	159.828	54.24	48591
2.141	39.8	155.875	52.90	48592
1.960	34.2	133.673	54.13	44484
*1.960	5.4	136.722	55.36	44484
1.792	29.4	114.643	55.53	40671
1.639	25.0	97.199	56.28	37199
1.478	21.2	82.134	58.49	33545
1.326	17.5	67.465	59.69	30095
1.120	13.4	51.211	63.50	25419
.930	9.8	36.938	66.43	21107
	Run H4.5 at 108°F.			
4.100	17.9	457.344	42.01	130603
4.004	17.2	439.362	42.32	127545
3.886	16.2	413.714	42.30	123786
3.748	15.2	388.040	42.65	119390
3.559	14.0	357.225	43.55	113370
3.396	12.9	328.983	44.05	108177
3.275	11.9	303.321	43.67	104323
3.275	77.2	302.922	43.61	104323
3.123	71.3	279.614	44.27	99481
3.123	11.1	282.792	44.77	99481
2.976	10.2	259.683	45.27	94798
2.976	65.4	256.242	44.68	94798
2.807	59.3	232.151	45.50	89415
2.807	9.2	234.023	45.86	89415
2.638	8.2	208.362	46.23	84032
2.638	52.7	206.032	45.72	84032
2.468	47.3	184.711	46.83	78616
2.468	7.4	187.829	47.62	78616
2.287	6.4	162.170	47.88	72851
2.287	41.2	160.625	47.42	72851
2.114	36.2	140.882	48.68	67340
*2.114	5.7	144.208	49.83	67340
1.929	31.1	120.745	50.11	61447
1.741	26.0	100.608	51.25	55458
1.552	21.5	82.840	53.11	49438
1.350	17.0	65.072	55.13	43003
*1.127	12.9	48.883	59.43	35896
* .905	9.3	34.668	65.36	28825
	Run H4.5 at 140°F.			
4.099	17.3	441.762	40.26	147125
3.781	15.1	385.318	41.28	135711
3.511	13.2	336.572	41.82	126020
3.286	11.7	297.992	42.25	117944
3.286	75.6	295.300	41.87	117944
3.111	69.2	269.898	42.72	111663
3.111	10.7	272.312	43.10	111663
2.946	9.8	249.242	43.99	105741
2.946	63.2	246.377	43.49	105741
2.760	56.2	219.134	44.05	99064
2.760	8.7	221.065	44.44	99064
2.619	8.0	203.134	45.32	94003
2.619	51.6	201.230	44.90	94003
2.485	47.3	184.318	45.72	89194
2.485	7.4	187.750	46.57	89194
2.371	6.8	172.362	46.92	85102

(continued)

TABLE 10 (continued)

W $lb_m/sec.$	HT cm	$-\Delta P_f$ lb_f/ft^2	$f \times 10^4$	RE175
	Run H4.5 at 140°F. (continued)			
2.371	43.3	168.597	45.89	85102
2.226	39.0	151.697	46.87	79898
2.226	6.0	151.848	46.92	79898
2.077	34.7	134.742	47.82	74549
2.077	5.4	136.454	48.42	74549
1.925	30.7	119.009	49.20	69094
1.765	26.5	102.442	50.34	63351
1.601	23.0	88.636	52.97	57462
1.430	18.8	72.069	53.97	51363
1.220	14.8	56.276	57.90	43787
.984	10.8	40.502	64.04	35317
	Run H21 at 68°F.			
4.087	19.4	489.163	44.69	96665
3.910	18.2	458.353	45.76	92479
3.805	17.2	432.677	45.61	89995
*3.660	15.5	389.029	44.32	86565
*3.438	14.0	350.516	45.26	81314
3.187	12.5	312.003	46.88	75378
2.980	11.3	281.192	48.33	70482
2.980	73.1	281.036	48.30	70482
2.845	67.6	259.219	48.88	67289
2.845	10.5	260.652	49.15	67289
2.680	9.5	234.976	49.93	63387
2.680	61.5	235.021	49.94	63387
2.524	55.4	210.823	50.51	59697
*2.524	8.7	214.436	51.37	59697
2.381	7.8	191.328	51.51	56315
2.381	49.9	189.005	50.88	56315
2.228	44.8	168.774	51.89	52696
*2.228	7.0	170.788	52.51	52696
2.072	6.2	150.247	53.41	49006
2.072	39.5	147.750	52.53	49006
1.884	34.0	125.932	54.15	44560
1.718	29.5	108.082	55.89	40634
*1.542	25.0	90.231	57.92	36470
*1.392	21.4	75.950	59.82	32923
*1.199	17.2	59.289	62.95	28358
*1.000	13.1	42.995	65.62	23651
* .778	9.6	29.119	73.43	18400
	Run H21 at 103°F.			
4.045	18.0	452.386	41.87	129320
3.882	16.8	421.586	42.36	124109
3.661	15.2	380.519	42.99	117044
3.423	13.5	336.872	43.54	109435
3.189	11.9	295.806	44.05	101954
	(continued)			

W $lb_m/sec.$	HT cm	$-\Delta P_f$ lb_f/ft^2	$f \times 10^4$	RE175
	Run H21 at 103°F. (continued)			
3.189	77.4	296.502	44.15	101954
3.009	70.0	267.234	44.70	96199
3.009	10.9	270.140	45.18	96199
2.836	9.8	241.908	45.55	90668
2.836	63.2	240.340	45.25	90668
2.672	56.9	215.423	45.69	85425
2.672	8.8	216.242	45.87	84525
2.512	8.0	195.696	46.96	80309
2.512	51.5	193.982	46.55	80309
2.331	45.4	169.866	47.34	74523
2.331	7.0	170.032	47.39	74523
2.127	6.1	146.924	49.18	68001
2.127	39.2	145.290	48.63	68001
1.953	34.2	125.532	49.84	62438
1.768	29.3	106.168	51.43	56523
1.593	25.0	89.175	53.22	50929
1.399	20.5	71.393	55.24	44726
1.231	17.1	57.957	57.92	39357
1.012	13.4	43.335	64.08	32355
.723	9.0	25.947	75.17	23115
	Run H21 at 130°F.			
4.006	17.2	431.579	40.43	144014
3.821	15.9	398.195	41.01	137363
3.612	14.4	359.709	41.45	129850
3.383	12.9	321.222	42.20	121617
3.139	11.5	285.283	43.53	112846
3.139	74.1	282.455	43.10	112846
2.980	67.1	254.850	43.15	107130
2.980	10.4	257.061	43.52	107130
2.793	9.4	231.405	44.60	100407
2.793	60.3	228.034	43.95	100407
2.575	53.2	200.035	45.36	92570
2.575	8.3	203.183	46.07	92570
2.398	7.3	177.527	46.42	86207
2.398	46.8	174.796	45.70	86207
2.193	40.8	151.135	47.25	78837
2.193	6.4	154.436	48.28	78837
1.980	5.4	128.780	49.39	71175
1.980	34.8	127.473	48.89	71175
1.746	28.8	103.812	51.20	62764
1.573	24.7	87.603	53.23	56545
1.385	20.7	71.835	56.31	49787
1.183	16.9	56.856	61.08	42526
.918	12.5	39.511	70.50	33000
.906	12.1	37.935	69.49	32567
.671	9.1	26.109	87.19	24121

__ The data below this line or marked * was neglected in calculating Table 7.

TABLE 11
OBSERVED AND CALCULATED HEAT TRANSFER DATA

$St \times 10^3$	h	W	$T_{.05}$	ΔT_m	RE	$STPR \times 10^3$
			Water			
1.386	722.8	.535	136.2	85.12	30535	2.965
1.499	692.6	.474	140.5	85.76	28045	3.131
1.207	629.5	.535	128.8	79.98	28642	2.707
1.297	1278.4	1.011	140.3	56.37	59726	2.709
1.147	1236.5	1.106	124.9	66.75	57107	2.644
1.175	1744.5	1.523	139.7	45.21	89515.	2.465
1.016	1566.2	1.581	117.5	55.37	76181	2.461
1.058	2167.0	2.101	140.3	37.25	124122	2.210
0.957	1937.1	2.076	113.6	44.16	96384	2.383
1.002	2515.0	2.575	135.0	33.07	145466	2.162
0.916	2306.6	2.582	114.5	38.65	120892	2.265
0.964	2884.4	3.068	133.0	29.61	170320	2.106
0.860	2576.4	3.074	111.5	35.55	139782	2.174
0.903	3043.5	3.455	134.1	27.50	193634	1.960
0.788	2813.1	3.660	109.8	32.60	163601	2.015
0.863	3462.5	4.114	131.5	25.14	225491	1.901
0.738	2966.2	4.120	107.2	30.94	179514	1.921
			Run L10			
0.796	2987.6	4.071	107.2	27.99	106647	2.072
0.852	2857.7	3.636	108.3	29.49	95614	2.200
0.917	2632.4	3.111	109.8	32.06	82238	2.345
0.961	2410.6	2.721	111.2	34.49	72275	2.433
1.012	2134.8	2.288	114.1	38.96	61363	2.511
0.964	1645.8	1.852	119.1	48.02	50528	2.306
0.996	1354.8	1.475	124.8	57.64	41013	2.295
1.044	1047.5	1.088	132.4	69.76	31023	2.290
1.146	655.3	.620	138.7	83.99	18047	2.420
			Run L20			
0.879	3112.5	3.990	108.4	26.63	91471	2.266
0.907	2988.1	3.714	108.0	27.40	84931	2.346
0.961	2782.0	3.263	109.6	29.72	75367	2.457
1.003	2555.5	2.871	111.1	31.88	66928	2.540
1.056	2247.6	2.398	114.6	36.22	57156	2.607
1.035	1898.8	2.068	119.1	43.60	50689	2.475
1.060	1937.6	2.060	120.1	43.37	50809	2.522
0.971	1516.1	1.759	119.8	52.33	43308	2.314
0.973	1318.1	1.527	123.7	56.65	38523	2.260
1.006	1190.1	1.333	129.0	63.86	34714	2.256
0.999	983.4	1.109	133.4	72.01	29686	2.178
1.022	721.8	.796	137.0	81.59	21771	2.182
1.085	557.5	.579	140.7	89.20	16206	2.266

(continued)

TABLE 11 (continued)

$St \times 10^3$	h	W	$T_{.05}$	ΔT_m	Re	$STPR \times 10^3$
			Run L30			
0.942	2891.8	3.703	107.5	29.70	68861	2.444
0.913	2971.9	3.926	106.7	28.76	72675	2.384
0.952	2802.9	3.552	107.7	30.29	66115	2.470
0.960	2613.5	3.286	108.6	32.14	61504	2.471
0.984	2474.2	3.035	110.8	35.42	57547	2.500
0.992	2302.6	2.800	112.1	37.99	53498	2.495
0.969	2073.9	2.582	114.0	41.55	49868	2.404
0.957	1877.6	2.367	117.4	45.95	46648	2.318
0.919	1668.5	2.190	120.1	50.94	43845	2.186
0.875	1447.8	1.997	122.6	57.13	40566	2.047
0.854	1294.5	1.829	124.9	61.53	37649	1.968
0.834	1120.6	1.622	127.5	72.28	33890	1.889
0.812	959.9	1.427	131.9	78.11	30568	1.785
0.770	743.2	1.164	134.3	85.63	25294	1.668
0.743	599.9	.974	136.9	92.61	21470	1.586
0.757	352.7	.562	142.3	107.09	12767	1.564
			Run L35			
0.932	2991.5	3.939	109.1	28.80	71546	2.391
0.972	3119.8	3.923	114.5	27.61	73721	2.404
0.976	2937.6	3.684	113.6	28.67	68879	2.430
0.970	2936.0	3.705	109.4	29.74	67579	2.484
0.995	2799.7	3.444	110.3	30.71	62860	2.532
1.071	3026.4	3.460	113.3	30.68	64581	2.671
1.025	2691.4	3.213	114.7	31.75	60461	2.530
1.021	2682.8	3.216	113.0	32.44	59926	2.551
1.056	2570.3	2.978	113.7	33.52	55716	2.625
1.045	2336.0	2.737	115.4	36.63	51715	2.566
1.046	2166.0	2.535	115.4	38.78	47899	2.569
1.030	1925.1	2.287	118.6	43.80	44026	2.472
0.991	1649.4	2.037	121.4	49.56	39852	2.336
0.968	1611.7	2.037	120.9	50.72	39739	2.290
0.943	1372.7	1.781	123.7	58.12	35319	2.190
0.897	1096.6	1.496	128.5	69.08	30488	1.976
0.861	849.0	1.207	132.2	79.28	25126	1.889
0.790	777.8	1.207	122.1	71.61	23714	1.855
0.779	618.8	.973	129.8	83.55	20525	1.831
0.847	672.7	.973	134.5	87.65	19984	1.737
			Run H4.5			
0.719	2673.1	3.909	103.3	34.14	121906	1.927
0.729	2601.6	3.755	103.4	34.48	117147	1.949
0.748	2553.0	3.592	103.8	34.76	112235	1.999
0.768	2512.3	3.440	104.5	36.06	107787	2.040
0.791	2466.8	3.280	105.1	36.82	103022	2.091
0.781	2323.5	3.129	105.4	38.02	98392	2.058
0.803	2237.3	2.932	105.9	39.13	92376	2.110
0.829	2140.8	2.716	106.8	40.64	85874	2.164

(continued)

TABLE 11 (continued)

St $x10^3$	h	W	$T_{.05}$	ΔT_m	RE	STPR$x10^3$
			Run H4.5 (continued)			
0.856	2078.8	2.555	108.1	42.71	81192	2.214
0.882	1974.9	2.356	108.7	43.72	75050	2.270
0.879	1798.9	2.154	111.3	48.43	69610	2.222
0.908	1720.4	1.994	112.8	50.66	64538	2.272
0.942	1587.0	1.772	114.7	54.87	57779	2.325
1.030	1471.2	1.503	117.7	57.97	49581	2.494
1.130	1342.0	1.250	121.7	63.47	41875	2.659
1.237	1134.5	.965	128.1	71.82	33123	2.791
			Run H21			
0.726	2549.7	4.035	101.5	32.62	128149	1.972
0.769	2609.8	3.901	101.7	32.67	124008	2.086
0.798	2567.4	3.699	104.7	34.71	119164	2.116
0.797	2563.5	3.699	105.4	34.04	119540	2.100
0.804	2469.7	3.530	106.2	34.79	114480	2.109
0.803	2419.1	3.352	107.6	35.45	109375	2.160
0.848	2288.7	3.103	108.7	37.38	101742	2.182
0.881	2241.5	2.927	109.9	38.27	96475	2.249
0.909	2162.2	2.734	111.7	40.20	90830	2.294
0.937	2029.2	2.491	112.2	43.60	82936	2.353
0.976	1940.7	2.287	114.4	48.29	76886	2.418
1.010	1993.1	2.269	117.8	50.33	77410	2.442
1.020	1838.5	2.072	114.1	48.70	69564	2.531
1.015	1617.4	1.832	116.0	52.32	62012	2.484
1.053	1469.5	1.604	118.1	57.47	54794	2.537
1.145	1369.6	1.376	122.7	63.13	47948	2.674
1.236	1226.1	1.141	128.7	69.11	40791	2.778
1.356	1055.3	.895	133.9	75.83	32711	2.944
1.519	787.0	.596	138.7	83.14	22228	3.208
1.343	1309.8	1.191	164.0	41.68	49281	2.440
1.511	591.4	.481	184.9	48.03	21622	2.470

T1	T2	T3	T4	T5	T6	T7	T8	TB1	TB2	W	CPE
					Run H21 High Temperatures ---Separation						
188.0	182.0	197.0	195.0	189.0	185.0	174.5	171.0	133.4	153.0	1.191	0.840
212.4	209.0	217.0	216.0	211.0	208.6	200.0	200.0	148.2	173.6	0.481	0.835
					Run L10						
144.6	135.2	138.5	127.6	123.4	116.3	98.9	98.4	89.4	97.2	4.071	0.946
146.6	136.8	141.8	130.2	125.5	117.6	99.7	99.3	89.2	98	3.636	0.946
150.0	139.0	147.0	134.0	128.1	121.0	100.8	100.5	88.7	99.0	3.111	0.946
152.4	141.1	151.8	138.0	130.6	123.9	102.0	101.4	88.2	99.8	2.721	0.946
156.5	144.6	160.9	144.6	136.9	130.1	104.8	104.0	87.8	101.6	2.288	0.946
161.5	148.7	177.7	155.6	151.2	144.6	109.0	108.2	87.0	103.2	1.852	0.946
170.5	156.0	187.0	164.5	165.7	156.5	121.0	118.4	86.0	106.1	1.475	0.946
180.0	167.0	192.3	175.7	174.0	165.1	147.3	144.0	84.8	110.3	1.088	0.946
190.7	180.5	197.8	187.2	187.6	180.0	166.0	161.3	79.9	113.6	.620	0.946

TABLE 11 (continued)

T1	T2	T3	T4	T5	T6	T7	T8	TB1	TB2	W	CPE
						Water					
190.0	179.0	189.0	184.0	185.5	176.5	167.0	164.0	73.0	114.3	0.535	1.000
193.0	184.0	193.0	188.4	190.3	180.3	173.0	170.0	75.2	120.0	0.474	1.000
187.5	179.5	187.5	181.2	183.0	174.0	134.0	136.0	72.0	105.8	0.535	1.000
178.7	168.0	180.0	172.8	176.0	165.0	158.0	154.4	99.4	125.0	1.011	1.000
179.3	167.7	181.3	171.3	176.0	166.3	160.0	150.5	101.4	127.2	1.000	1.000
174.5	160.5	177.0	163.0	171.0	158.0	137.0	133.5	78.2	105.0	1.106	1.000
175.0	163.0	176.8	163.0	169.5	161.5	149.1	146.0	107.8	126.4	1.523	1.000
166.0	152.5	170.0	153.0	154.0	145.5	117.0	115.0	80.0	99.7	1.581	1.000
171.0	161.0	173.7	162.0	167.0	158.5	143.6	140.7	114.8	128.6	2.101	1.000
169.7	159.0	172.3	158.5	164.5	156.0	140.5	138.3	111.5	126.0	2.000	1.000
160.5	147.0	158.0	141.5	142.5	136.0	107.5	106.0	84.2	99.0	2.076	1.000
166.0	156.0	168.0	153.6	159.0	151.6	134.0	131.6	112.7	124.3	2.575	1.000
156.5	144.0	154.0	138.5	140.5	134.5	108.0	106.5	89.0	101.4	2.582	1.000
163.5	154.0	162.7	149.5	154.2	148.4	129.8	128.3	113.2	123.2	3.068	1.000
153.0	140.5	148.0	134.0	135.0	130.0	103.5	102.5	88.4	99.1	3.074	1.000
163.7	153.2	161.5	150.0	154.2	148.5	130.3	129.0	116.0	124.7	3.455	1.000
150.0	138.0	143.0	131.0	131.0	126.0	101.5	100.5	89.0	98.0	3.660	1.000
159.5	151.5	156.5	146.0	150.0	145.0	127.0	125.5	115.2	122.8	4.114	1.000
146.0	135.0	140.5	127.0	127.0	122.0	098.5	098.0	87.8	95.8	4.120	1.000
						Run L30					
148.0	138.0	140.0	132.2	122.6	114.5	98.9	98.9	87.8	97.6	3.703	0.850
146.5	137.0	138.0	130.6	121.8	113.2	98.0	98.0	87.8	97.0	3.926	0.850
148.5	138.5	141.0	133.0	123.5	115.0	99.0	99.0	87.6	97.7	3.552	0.850
150.1	139.3	145.0	136.0	126.0	117.1	99.2	99.2	87.2	98.0	3.286	0.850
152.4	141.4	150.0	141.0	131.0	122.6	101.6	101.6	87.0	99.2	3.035	0.850
154.8	143.6	154.2	145.2	133.7	126.6	102.5	102.5	86.6	99.8	2.800	0.850
157.4	146.0	159.6	150.6	139.3	132.0	103.8	103.1	86.2	100.3	2.582	0.850
160.5	148.5	166.2	157.2	147.5	141.4	108.0	106.5	86.8	102.2	2.367	0.850
165.4	152.0	171.0	162.0	156.0	149.5	111.0	110.0	86.5	102.9	2.190	0.850
171.0	158.5	178.0	169.0	162.0	152.6	115.6	115.0	85.3	102.8	1.997	0.850
175.0	163.0	183.0	174.0	167.6	155.6	120.3	119.5	85.0	103.4	1.829	0.850
179.7	170.0	187.0	182.0	170.0	159.0	138.5	134.0	80.9	102.0	1.622	0.850
185.5	175.5	192.0	187.0	176.0	165.0	150.0	146.0	81.8	104.0	1.427	0.850
190.0	182.0	195.0	191.0	182.5	173.0	158.0	154.0	80.0	103.1	1.164	0.850
195.0	188.0	198.0	196.5	189.0	181.0	165.0	161.0	78.6	102.7	0.974	0.850
204.0	199.0	204.0	204.0	201.0	195.0	183.0	182.0	74.6	103.0	0.562	0.850
						Run L20					
145.0	135.6	138.5	128.0	122.7	116.3	100.1	100.1	91.0	99.2	3.990	0.910
146.2	136.5	139.5	128.5	121.8	116.0	99.3	99.3	90.0	98.7	3.714	0.910
148.3	138.0	143.4	132.6	125.0	119.3	101.2	101.2	89.8	99.8	3.263	0.910
151.0	140.5	146.8	136.0	128.0	121.8	103.0	102.6	89.6	100.8	2.871	0.910
155.0	144.0	155.5	143.5	136.0	129.0	105.7	105.7	89.8	103.2	2.398	0.910
160.0	148.0	171.0	154.0	147.0	140.3	109.5	109.1	89.4	105.2	2.068	0.910
160.3	148.5	171.5	154.4	148.0	142.2	110.8	110.2	90.4	106.5	2.060	0.910

(continued)

TABLE 11 (continued)

T1	T2	T3	T4	T5	T6	T7	T8	TB1	TB2	W	CPE
					Run L20 (continued)						
164.5	151.2	181.0	160.0	156.0	150.0	109.1	108.2	84.8	102.6	1.759	0.910
170.1	157.5	185.0	166.1	165.3	156.0	114.6	113.8	85.8	105.1	1.527	0.910
177.3	164.5	188.0	173.5	170.7	160.5	133.7	129.5	85.9	108.4	1.333	0.910
183.0	171.7	191.0	180.0	176.0	167.3	149.0	145.0	84.8	110.0	1.109	0.910
189.2	181.0	195.0	187.0	184.5	177.0	159.7	156.5	81.7	110.9	0.796	0.910
194.0	187.2	197.0	192.7	192.0	185.4	171.0	168.5	79.2	113.1	0.579	0.910
					Run L35						
147.3	137.0	139.7	132.0	124.7	118.4	101.0	100.6	90.0	99.4	3.929	0.838
150.4	140.4	146.2	136.4	128.8	123.0	106.6	106.6	96.0	105.4	3.923	0.839
150.4	140.4	146.2	136.8	128.6	122.6	105.7	105.3	94.4	104.2	3.684	0.838
148.3	137.7	142.2	133.5	124.7	118.4	101.4	101.0	89.5	99.6	3.705	0.838
149.6	139.0	145.4	134.5	126.1	120.0	102.3	101.4	89.6	100.3	3.444	0.838
151.4	140.7	148.0	137.7	129.7	124.0	105.3	105.3	92.3	103.8	3.460	0.838
152.4	142.3	151.0	140.5	132.2	126.4	106.6	106.0	93.2	104.6	3.213	0.838
152.2	141.2	150.0	139.3	131.0	124.7	104.4	103.8	91.0	102.6	3.216	0.838
153.8	143.0	153.0	141.8	131.4	125.1	104.8	104.4	90.8	103.2	2.978	0.838
156.0	145.0	157.5	146.2	136.0	130.0	106.0	106.0	90.4	103.8	2.737	0.838
157.7	146.0	159.0	148.0	138.0	131.4	106.0	106.0	89.0	103.2	2.535	0.838
161.0	148.7	166.0	155.0	147.5	141.4	108.5	108.0	88.8	104.6	2.287	0.838
165.3	152.0	172.0	161.0	157.7	150.4	112.0	111.0	88.1	105.3	2.037	0.838
165.3	152.0	172.0	160.6	157.7	151.2	112.0	111.0	87.0	104.2	2.037	0.838
172.0	158.5	178.4	167.0	165.0	155.0	120.5	117.4	85.1	104.3	1.781	0.838
180.5	168.5	187.0	175.7	171.7	161.0	137.7	133.0	83.2	104.9	1.496	0.838
186.0	175.7	193.0	183.6	179.0	170.0	151.0	145.5	80.7	104.6	1.207	0.838
183.6	176.0	190.0	180.7	179.5	163.7	104.0	104.0	76.4	96.2	1.207	0.837
189.0	182.5	193.0	186.0	184.0	176.5	137.0	137.0	76.7	99.5	0.973	0.837
191.0	183.7	193.0	189.0	186.8	178.0	159.0	154.0	77.7	103.7	0.973	0.837
					Run H4.5						
144.6	133.5	137.5	132.3	120.0	110.0	91.5	91.5	81.5	88.6	4.116	0.975
146.0	135.0	141.5	135.0	122.5	112.5	93.0	92.5	82.0	90.6	3.909	0.975
146.6	135.6	143.0	135.0	122.5	112.0	93.0	92.5	81.8	90.6	3.755	0.975
147.5	136.0	143.4	135.6	124.0	112.5	93.0	92.5	81.9	91.0	3.592	0.975
148.7	137.0	145.0	138.5	125.0	114.5	93.5	93.5	81.7	91.4	3.440	0.975
149.5	137.7	146.0	140.0	126.8	115.5	94.0	93.5	81.6	91.8	3.280	0.975
150.5	138.5	147.0	143.8	127.2	116.0	94.0	93.5	81.2	91.6	3.129	0.975
151.6	139.7	148.0	144.6	128.5	117.4	95.0	94.6	80.9	91.9	2.932	0.975
153.0	141.0	151.0	147.5	130.6	119.7	95.0	94.6	80.6	92.4	2.716	0.975
155.0	142.2	153.0	151.6	134.0	122.6	96.7	96.0	80.4	93.2	2.555	0.975
156.5	144.0	155.0	153.6	135.0	123.0	96.7	96.3	80.1	93.6	2.356	0.975
158.5	146.7	163.4	162.0	141.4	130.0	99.0	98.5	79.7	94.6	2.154	0.975
160.0	148.0	166.5	165.0	145.2	135.0	100.3	100.0	79.5	95.6	1.994	0.975
163.0	151.0	169.5	167.3	151.6	143.4	103.6	102.0	78.3	96.4	1.772	0.975
166.0	154.4	172.5	171.0	157.2	149.0	108.2	108.2	78.3	99.2	1.503	0.975
170.0	158.0	176.5	175.7	164.0	156.0	120.0	118.6	77.5	102.6	1.250	0.975
175.7	164.7	182.5	181.5	171.8	163.0	142.5	138.0	76.7	107.8	0.965	0.975

(continued)

TABLE 11 (continued)

T1	T2	T3	T4	T5	T6	T7	T8	TB1	TB2	W	CPE
					Run H21						
145.5	135.1	136.4	130.8	119.0	109.0	91.5	91.0	81.1	89.4	4.035	0.892
145.7	135.3	136.8	131.0	119.2	109.4	91.5	91.0	81.0	89.8	3.901	0.892
148.3	137.8	142.0	136.2	124.0	113.8	95.0	94.2	82.5	92.2	3.699	0.892
148.3	138.2	142.5	137.0	124.0	114.2	95.4	95.0	83.7	93.2	3.699	0.892
150.0	140.0	144.1	138.5	125.0	115.0	96.0	96.0	84.0	93.8	3.530	0.892
151.0	140.5	147.0	141.5	127.0	117.0	97.0	97.0	84.8	95.1	3.352	0.892
152.4	142.2	150.0	144.5	129.8	119.3	98.0	98.0	84.5	95.6	3.103	0.892
154.0	143.4	152.0	146.6	131.8	121.0	100.0	98.5	84.9	96.7	2.927	0.892
155.6	145.0	155.0	151.6	135.0	125.0	101.0	100.6	85.7	98.0	2.734	0.892
157.7	146.2	158.0	156.8	138.5	127.7	101.0	101.0	83.3	97.6	2.491	0.892
159.7	148.3	164.0	163.0	144.9	136.2	103.6	103.0	82.1	98.6	2.287	0.892
161.3	149.1	167.5	166.5	152.2	143.4	108.6	107.4	83.8	101.6	2.269	0.892
161.0	149.5	165.0	164.0	144.0	134.0	103.0	102.0	81.1	98.5	2.072	0.892
163.0	152.4	170.0	169.0	149.5	139.0	105.0	104.0	80.6	99.2	1.832	0.892
165.5	155.0	174.0	173.0	156.5	149.0	108.0	107.0	78.8	100.0	1.604	0.892
169.5	159.5	178.0	178.0	166.0	156.0	120.0	118.0	78.5	103.8	1.376	0.892
174.0	164.5	182.0	182.5	172.0	163.0	139.0	136.4	79.2	109.1	1.141	0.892
180.0	171.5	186.5	187.5	178.0	170.0	156.0	150.5	78.0	114.0	0.895	0.892
187.5	180.5	193.0	193.5	187.0	180.0	166.0	160.0	75.1	119.3	0.596	0.892

Table 12. Physical Properties of Oils (Ward)

Temperature °F.	Light Oil Density lb/ft^3	Light Oil Viscosity Centipoise	Heavy Oil Density lb/ft^3	Heavy Oil Viscosity Centipoise
62	53.87	18.2	55.32	261
64	53.79	17.2	55.28	245
66	53.76	16.4	55.25	229
68	53.73	15.6	55.22	214
70	53.67	14.7	55.19	196
72	53.64	13.9	55.16	181
74	53.57	13.0	55.13	162
108	52.86		54.26	
140	52.23		53.64	

Temperature °F	Light Oil Heat Capacity BTU/lb°F.	Light Oil Thermal Conductivity BTU/lb°F., ft	Heavy Oil Heat Capacity BTU/lb°F.	Heavy Oil Thermal Conductivity BTU/lb°F., ft
100	0.450	0.077	0.448	0.074
300	0.560	0.076	0.559	0.071

Table 13. Density of Manometer Fluids (Ward)

Temperature °F	2.94 Sp. Gr. Oil lb/ft^3	Mercury lb/ft^3
68	120.91	782.59
69	120.84	782.53
70	120.77	782.47
71	120.70	782.41
72	120.62	782.35
73	120.55	782.29
74	120.48	782.23
75	120.41	782.17
76	120.34	782.11
77	120.26	782.05
78	120.19	781.99
79	120.12	781.93
80	120.05	781.87
81	119.98	781.81
82	119.90	781.75
83	119.83	781.69
84	119.76	781.63
85	119.69	781.57

FRICTION LOSS IBM PROGRAM

```
      DIMENSION W(99), PF(99). REVIS(99), FF(99), RE(99), RE175(99), RE180(99)
100   FORMAT (12, 2X, F4.4, 2X, F5.3)
101   FORMAT (F4.3, 2X. F3.1, 2X, F5.2, 2X, F5.4, 2X, F5.3, 2X, F5.3)
102   FORMAT (52H  W        PF          FF          RE      RE175       RE180 / )
103   FORMAT (4X, F8.5, 1X, F8.5, 1X, F8.4, 1X, F8.5, 1X, 4(F8.4, 1X) )
104   FORMAT (F8.3, 1X. F8.3, 1X, F8.6, 1X, 3(F8.0, 1X) )
105   FORMAT (///75H       SLOPE    ERROR    Y-INTER    ERROR    Y-180     VI
     1S180       U-175       VIS175/)
  7   READ 100, N, DE, P
      PUNCH 102
      CRE = 1488.*12. /(.7853982*DE )
      CFF = 9.8696044  *  32.172  *  (DE/12.)**5./192.
      SUMX = 0
      SUMY = 0
      SUMXY = 0
      SUMXX = 0
      SUMYY = 0
      AAA = .328083E-1
      DO 5  I=1,N
  1   READ 101, W(I), HT, PM, VIS, PE, PW
      PF(I) = AAA*HT*PM + 6. (PE-PW)
      FF(I) = CFF*PF(I)*PE/(W(I)*W(I) )
      REVIS (I) = CRE*W(I)
      RE(I) = REVIS (I)/VIS
      X=LOGF(W(I))
      Y=LOGF(PF(I))
      XY=X*Y
      XX=X*X
      YY=Y*Y
      SUMX=SUMX+X
      SUMY=SUMY+Y
      SUMXY=SUMXY+XY
      SUMXX=SUMXX+XX
  5   SUMYY=SUMYY+YY
      AN=N
      SXX = SUMXX - (SUMX*SUMX)/AN
      SYY = SUMYY - (SUMY*SUMY)/AN
      SXY = SUMXY - (SUMX*SUMY)/AN
      SLOPE = SXY/SXX
 10   SYXSQ = (SYY-SLOPE*SLOPE*SXX)/(AN-2.)
      SBSQ = SYXSQ/SXX
      SB = SQRTF(SBSQ)
      ALN = (SUMXX*SUMY-SUMX*SUMXY)/(AN*SXX)
      ALN18 = (SUMY - 1.8*SUMX)/AN
      ALN17 = (SUMY - 1.75*SUMX)/AN
 15   A = EXPF(ALN)
      SA = SQRTF(SYXSQ/AN + SUMX*SUMX*SBSQ/(AN*AN))
 20   ERRORA = EXPF(ALN+SA)/2. - EXPF(ALN-SA)/2.
```

(continued)

FRICTION LOSS IBM PROGRAM (continued)

```
      A175 = EXPF(ALN17)
      A180 = EXPF(ALN18)
      C4 = 1488.  **  .2
      C5 = 4.  *  .2
      C7 = 4.  **.25
      C6 = 1488.**.25
      C17 = .079*192./(C6*C7*3.1415927**1.75*32.172*(DE/12.)**4.75)
      C18 = .046 *192./(C4*C5 * 3.1415927**1.8*32.172 *(DE/12.)**4.8)
      VIS180  =  (A180*P/C18)**5.
      VIS175  =  (A175*P/C17)**4.
      DO 21 I = 1, N
      RE175(I) = REVIS(I)/VIS175
      RE180(I) = REVIS(I)/VIS180
21    PUNCH 104, W(I), PF(I), FF(I), RE(I), RE175(I), RE180(I)
      PUNCH 105
      PUNCH 103, SLOPE, SB, A, ERRORA, A180, VIS180, A175, VIS175
      GO TO 7
      END
```

HEAT TRANSFER PROGRAM

```
      INPUT          T1  TO  T8,  TB1, TB2, W, CPE

      OUTPUT         ST, REVIS, H,  W,  TO5, DTM

101   FORMAT (10(F4. 1, 2X), 2(F4. 3, 2X) )
102   FORMAT (F8. 6, F8. 0, F8. 1, F8. 3, F8. 1, F8. 2)
103   FORMAT (47H      ST      REVIS      H         W         T05         DTM//)
 20   PUNCH 103
  1   READ 101, T1, T2, T3, T4, T5, T6, T7, TB1, TB2, W, CPE
      TA=(T1+T2)/2.
      TB=(T3+T4)/2.
      TC=(T5+T6)/2.
      TD=(T7+T8)/2.
      DTB=TB2=TB1
  2   TL1 = 5.
      TL2 = 24.
      TL3 = 41.
      TL4 = 63.
  3   TM1 = TB1 + DTB*TL1/72.
      TM2 = TB1 + DTB*TL2/72.
      TM3 = TB1 + DTB*TL3/72.
      TM4 = TB1 + DTB*TL4/72.
  4   A = TL1/144.
      B = (TL2-TL1)/144.
      C = (TL3-TL2)/144.
      D = (TL4-TL3)/144.
      E = (72.-TL4)/144.
  5   TAA = TA-TB1 + TA - TM1
      TBB = TA - TM1 + TB = TM2
      TCC = TB - TM2 + TC - TM3
      TDD = TC - TM3 + TD = TM4
      TEE = TD -  TM4 + TD - TB2
  6   DTM = A*TAA+B*TBB+C*TCC+D*TDD+E*TEE
      AA = 2784. 728
  7   H = AA*W*CPE*DTB/DTM
      BB = .00285764
      CC = 27624. 5
  8   ST = BB*DTB/DTM
  9   REVIS = CC*W
      TO5 + (TB1 + TB2 + DIM)/2.
      PUNCH 102, ST, REVIS, H, W, TO5, DIM
      IF(SENSE SWITCH 9) 10, 1
 10   GO TO 20
      END
```

```
      LEAST SQUARE          HEAT TRANSFER
      INPUT          PR = CP*VIS/K  AT  TOS  FOR  WATER
      INPUT          VIS  AT  TOS  FOR THE DISPERSION  ST, RE, PR
      DIMENSION RE(99), STPR(99)
  100 FORMAT (I2)
  101 FORMAT (F6.6, 2X, F6.0, 2X, F3.2)
  102 FORMAT (F8.6, 2X, F8.6, 2X, F8.5, 2X, F8.6, 2X, F8.5)
  103 FORMAT (//45H   SLOPE     ERROR      A1         ERROR       A2/)
  104 FORMAT (F8.0, F8.6)
  105 FORMAT (14H    RE       STPR/)
    7 PUNCH 105
      SUMX = 0
      SUMY = 0
      SUMXY = 0
      SUMXSQ = 0
      SUMYSQ = 0
      READ 100, N
      DO  5 I = 1, N
   10 READ 101, ST, RE(I), PR
      STPR(I) = ST*PR**.666667
      PUNCH 104, RE(I), STPR(I)
    5 CONTINUE
      DO 29 I = 1, N
      Y = LOGF(STPR(I))
      X = LOGF(RE(I))
      XY = X*Y
      XSQ = X*X
      YSQ = Y*Y
      SUMX = SUMX+X
      SUMY = SUMY+Y
      SUMXY = SUMXY+XY
      SUMXSQ = SUMXSQ+XSQ
   29 SUMYSQ = SUMYSQ+YSQ
   30 AN = N
      SXX = SUMXSQ - (SUMX*SUMX)/AN
      SYY = SUMYSQ - (SUMY*SUMY)/AN
      SXY = SUMXY - (SUMX*SUMY)/AN
   26 SLOPE = SXY/SXX
      SYXSQ = (SYY-SLOPE*SLOPE*SXX)/(AN-2.1)
      SBSQ = SYXSQ/SXX
   27 SB = SQRTF(SBSQ)
      ALN1 = (SUMXSQ*SUMY-SUMX*SUMXY)/(AN*SXX)
      ALN2 = (SUMY + .2*SUMX)/AN
      SALN = SQRTF(SYXSQ/AN + SUMX*SUMX*SBSQ/(AN*AN))
      A1 = EXPF(ALN1)
      A2 = EXPF(ALN2)
      ER1 = ALN1 + SALN
      ER2 = ALN1 - SALN
      SA = EXPF(ER1)/2. - EXPF(ER2)/2.
      PUNCH 103
      PUNCH 102, SLOPE, SB, A1, SA, A2
      GO TO 7
      END
```

NOMENCLATURE

Symbol	Meanings	Dimensions
A	Cross sectional area of test section	ft^2
A_n, A_m	Constants	
B	Constants	
C, C_n	Constants	
Cp	Heat capacity of water	BTU/lb,°F.
Cpe	Heat capacity of dispersion	BTU/lb,°F.
D	Diameter of tube	inches or feet
f	Friction factor	
g	Acceleration of gravity	ft/sec^2
g_c	Gravitational constant, 32.172	$lb_m/ft/lb_f, sec^2$
G	Mass flow rate	lb_m/ft^2-sec
HT	Deflection on function pressure loss measuring manometer	centimeters
h	Heat transfer coefficient	BTU/hr,ft^2, °F
j_H	Colburn's factor for heat transfer	
k	Thermal conductivity	BTU/hr,ft^2, °F
K	Conversion for obtaining feet	
L	Length of test section	feet or inches
$\overline{lw}$	Work lost due to friction	$ft, lb_f/lb_m$
n	Exponial constant, power law model	
Nu	Nusselt number, h D/k	lb/in^2
P_f	Friction pressure	lb/in^2

Symbol	Meanings	Dimension
ΔP_s	Static pressure difference	lb/in^2
ΔP_T	Pressure drop across test section	lb/in^2
ΔP_f	Pressure difference due to friction losses	lb/in^2
Pr	Prandtl number, hD/k	
Pr_c	Prandtl number of continuous phase	
Pr_w	Prandtl number at the wall temperature	
q	Amount of heat transferred	BTU/hr
Re	Reynolds number $D\rho V/\mu$	
Re_c	Renolds number of continuous phase	
St	Stanton number h/GCp	
T1 to T8	Temperature of 8 wall thermocouples	^oF
ΔT_b	Temperature rise of fluid, TB1-TB2	^oF
TB1	Inlet fluid temperature	^oF
TB2	Outlet fluid temperature	^oF
ΔT_m	Mean temperature difference	^oF
T_w	Wall temperature	^oF
T_b	Bulk fluid temperature	^oF
u, v, w	Point velocity in x, y, z direction	ft/sec
V	Average velocity	ft/sec
W	Mass flow rate	lb_m/sec
$\overline{w}$	Work done on fluid	$ft, lb_f/lb_m$

Symbol	Meaning	Dimensions
Y	Defined by equation (50)	
ΔZ	Change in height	feet
S_D	Error in h	
S_h	Error in h	
S_{HT}	Error in HT	
S_f	Error in f	
S_{PM}	Error in ρ_m	
$S_{(PE-PW)}$	Error in $\rho_e - \rho_w$	
S_{PE}	Error in ρ_e	
$S_{\Delta T_b}$	Error in ΔT_b	
$S_{\Delta T_m}$	Error in ΔT_m	
S_{RE}	Error in Re	
S_{St}	Error in St	
S_w	Error in W	
S_u	Error in μ	
	Greek Symbols	
ϵ, ϵ', m	Functions of f, see equation 10	
μ	Viscosity	centipoise
μ_c	Viscosity of continuous phase	centipoise
μ_d	Viscosity of dispersed phase	centipoise
μ_e	Effective viscosity of the dispersion	centipoise
ρ	Density	lb/ft^3
ρ_d	Density of dispersed phase	lb/ft^3

Symbol	Meaning	Dimensions
ρ_e	Density of dispersion	lb/ft^3
ρ_m	Density of manometer fluid	lb/ft^3
ρ_s	Density of dispersed phase	lb/ft^3
ρ_w	Density of water	lb/ft^3
ϕ	Volume fraction of dispersed phase	
$\frac{\partial}{\partial x}$	Partial derivative with respect to x	

Symbols Used in the Computer Printouts

A	least square y-intercept
C175	Constant, equation (44)
CPE	Cpe
CRE	Constant, equation (41)
CFF	Constants, equation (37)
DTB	ΔT_b
DTM	ΔT_m
FF	f
H	h
PF	ΔP_f
PE	ρ_e
PW	ρ_w
RE	Re
RE175	Re using an effective viscosity by fitting ΔP_f vs W to slope of 1.75

Symbols	Meaning
RE180	Re using an effective viscosity by fitting ΔP_f vs W to slope of 1.80
REVIS	(Re)μ
SA	Error on A
SB	Error on slope
SLOPE	Least square slope
ST	St
STPR	$(St)(Pr)^{2/3}$
T05	$T_{0.5}$
VIS	Viscosity
VIS175	Effective viscosity used in RE175
VIS180	Effective viscosity used in RE180